

Grant agreement no.:

101060634

Project acronym:

PURPEST

Project full title:

Plant pest prevention through technology-guided monitoring and site-specific control

Collaborative Project (RIA Research and Innovation action)

HORIZON EUROPE CALL – HORIZON-CL6-2021-FARM2FORK-01

Start date of project: 2023-01-01

Duration: 4 years

D 3.2

Report on functional testing performance of Sensor System Prototype

Due delivery date: 31-05-2025

Actual delivery date: 03-06-2025

Organization name of lead contractor for this deliverable:

SINTEF

Project co-funded by the European Commission within HORIZON 2020 (2016-2020)		
Dissemination Level		
PU	Public, fully open, e.g. web	X
CO	Confidential, restricted under conditions set out in Model Grant Agreement	
CI	Classified, information as referred to in Commission Decision 2001/844/EC.	

Deliverable number:	D3.2 / D12
Deliverable name:	Report on functional testing performance of Sensor System Prototype
Work package:	WP3
Lead contractor:	SIN

Author(s)		
Name	Organisation	E-mail
Daniel Nilsen Wright	SIN	daniel.nilsen.wright@sintef.no
Karolina Milenko	SIN	karolina.milenko@sintef.no
Knut Thorshaug	SIN	knut.thorshaug@sintef.no
Damien Bazin	AIRMO	damien.baazin@chromatotec.com
Ali Ghaddar	AIRMO	ali.ghaddar@chromatotec.com
Stéphane Le Calvé	AIRMO	stephane.le-calve@chromatotec.com

Pavol Miškovský	Saftra Photonics	pavol.miskovsky@saftra-photonics.org
Usman Yaqoob	UWAR	Usman.yaqoob@warwick.ac.uk
Siavash Esfahani	UWAR	Siavash.esfahani@warwick.ac.uk
Julian W Gardner	UWAR	J.W.gardner@warwick.ac.uk
Marina Cole	UWAR	Marina.cole@warwick.ac.uk
Adomas Malaiska	VOL	Adomas@volatile.ai
Lucas Lopez	VOL	Lucas@volatile.ai

Abstract

This deliverable reports on the functional testing performance of the Sensor System Prototypes (SSPs) developed within the PURPEST project. Building on the component-level evaluations presented in D2.2, this report focuses on the integrated performance of the SSPs, combining results from partner-led laboratory tests and intercomparison campaigns, including the March 2025 evaluation at UNINE. The SSPs are designed to detect volatile organic compounds (VOCs) associated with pest-infested plants, including ethanol, 2-methyl-1-butanol, d-limonene, and (E)-2-hexenal. The systems tested include AIRMO's microVOC, VOL's Scout3, UWAR's μ -GC and SMR-based e-nose, SINTEF's SERS platforms, and SAFTRA's PickMol technology. While AIRMO and VOL systems demonstrated strong detection capabilities, other components showed promising developments but require further optimization. The results support the selection and refinement of SSPs for upcoming field trials and contribute to the development of a robust, field-deployable pest detection system.

Public introduction¹

This deliverable presents the results of functional testing of the Sensor System Prototypes (SSPs) being developed in the PURPEST project. The SSPs are designed to enable early detection of pest infestations in plants by identifying specific volatile organic compounds (VOCs) emitted during the early stages of infection. These systems are intended for use in customs inspections, agricultural monitoring, and other field applications to help protect plant health across the EU and EEA.

The report builds on earlier work that identified key VOCs linked to plant pest infestations. It evaluates the performance of complete sensor systems and their components, including gas chromatography units, photoionization detectors, micro-GC columns, solidly mounted resonators, and SERS-based detection platforms. Testing was conducted both at partner facilities and during a collaborative intercomparison campaign. The findings highlight the progress made in integrating these technologies into portable systems and identify areas for further improvement. This work is a key step toward deploying SSPs in real-world environments for sustainable and efficient pest management.

¹ According to Deliverables list in Annex I, all restricted (RE) deliverables will contain an introduction that will be made public through the project WEBSITE

TABLE OF CONTENTS

	Page
1 INTRODUCTION.....	4
2 IMPROVEMENT OF FIRST SSP	5
2.1 Description of AIRMO systems	5
2.2 Description of Volatile system	6
2.3 Description of UWAR system.....	7
2.3.1 UWAR micro-GC progress summary	7
2.3.2 Micro-GC modelling and simulation work.....	7
2.3.3 Design, fabrication, and testing of μ -GC columns	9
2.3.4 Publications to date on the micro-GC work	11
3 IMPROVEMENT OF THE INDIVIDUAL PARTS.....	12
3.1 Pre-concentration.....	12
3.2 Separation	12
3.2.1 3D-printed μ -GC.....	12
3.2.2 Miniature GC columns	12
3.3 Coating development for SERS and SMR	13
3.3.1 Introduction.....	13
3.3.2 Surface Metal-Organic Frameworks (SURMOFs).....	13
3.3.3 UWAR coatings progress summary	22
3.4 VOC detection	24
3.4.1 Solidly mounted resonators	24
3.4.2 Photoionization Detector	31
3.4.3 SERS.....	33
3.4.4 PickMol technology.....	38
4 CONCLUSION	44
5 REFERENCES	45

1 INTRODUCTION

This deliverable presents the results of the functional testing of the first generation of Sensor System Prototypes (SSPs) developed within the PURPEST project. The primary objective of this report is to evaluate the performance of these prototypes and their individual components under controlled conditions, as part of Task 3.3. The insights gained from this testing phase will guide the selection and refinement of SSPs for upcoming field trials.

The SSPs are designed to detect and quantify volatile organic compounds (VOCs) emitted by pest-infested plants, enabling early and precise pest detection in agricultural settings. The systems integrate a range of technologies including micro-gas chromatography (μ -GC), photoionization detectors (PID), solidly mounted resonators (SMRs), and surface-enhanced Raman scattering (SERS) platforms.

This report builds upon previous deliverables (D2.2 and D3.1), offering a comprehensive assessment of the SSPs' capabilities, limitations, and improvements. It also includes comparative analyses, simulation results, and experimental data that collectively inform the next steps in system integration and deployment.

A conceptual illustration of the SSP is given in Figure 1-1. It will be portable on the back of the operator with a sensing probe connected to the unit via a tube (not illustrated).

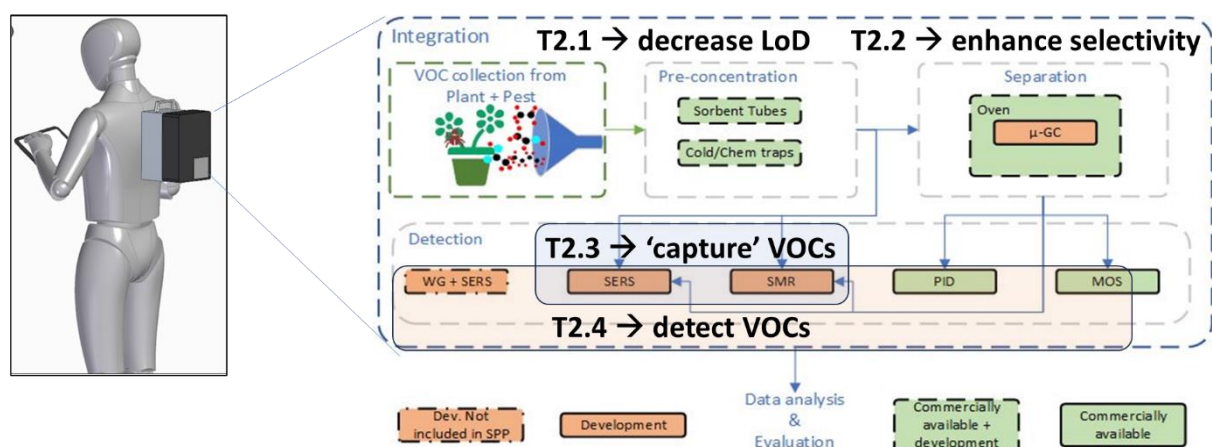


Figure 1-1: Conceptual illustration of the PurPest SSP and its base components for detection.

2 IMPROVEMENT OF FIRST SSP

2.1 Description of AIRMO systems

The first prototype of the sensor system has been extensively described in the Deliverable D3.1 (*First Sensor System Prototype – September 2024*). Developed and manufactured by AIRMO, the system was designed to detect and quantify Biogenic Volatile Organic Compounds (BVOCs) emitted by pest-infested plants. This portable unit integrates a pre-concentration module, an automatic injection valve, a heated chromatographic column, and a photoionization detector (PID), as illustrated in Figure 2-1.

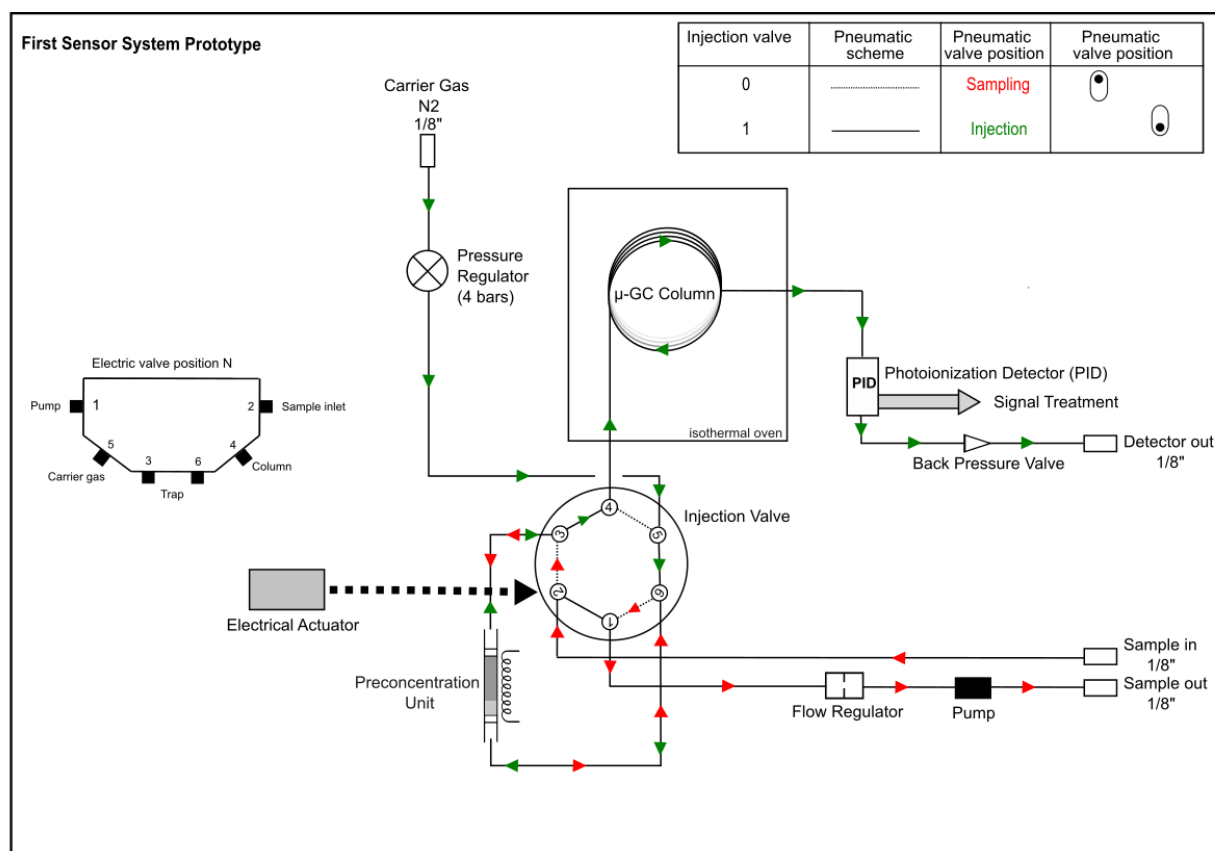


Figure 2-1: Pneumatic scheme of the first sensor system prototype.

During the inter-comparison held at AIRMO's facility on April 8, 2024, synthetic gas mixtures were produced to assess the sensitivity and specificity of the newly developed sensors and analyzers provided by the PurPest consortium. Detailed documentation and results are available in Deliverable D2.2 (*Report on Performance of Individual Sensor System Components – July 2024*). The AIRMO sensor demonstrated reliable detection and quantification of all targeted compounds with good repeatability at both ppm and ppb levels.

However, a key limitation of the first prototype was its inability to effectively quantify compounds with high boiling points, due to adsorption on the non-heated PID. To address this, AIRMO developed a heated PID and evaluated its performance by comparing the original prototype with a modified system equipped with the new heated PID and a gradient oven during a second inter-comparison at UNINE in March 2025 (developed in section 3.4.2.2).

2.2 Description of Volatile system

Scout3 (Figure 2-2) is an instrument developed by Volatile Technologies for volatile organic compound (VOC) measurements on the go. The system includes multiple gas detection sensor technologies, such as photoionization detectors (PID) and metal oxide (MOX) detectors and is easily adapted to include different sensor types and chambers. As a standard, there are three different ionization and sensitivity level PID detectors included, which provide a degree of separation of compounds. The system includes a gas chromatography (GC) column for further sample separation and its portable nature allows measurements on the field and at-line. The system has the ability to take a VOC sample using either dynamic or static headspace modes from a sealed glass vial for liquid and solid samples (such as plant leaves).

During the PURPEST project, the system has been adapted to also include an open-air inlet for measurements on the go from the environment. This can come in handy for future plant tests in the field. Further to that, a detailed review, design and improvement of electrical control systems and PCBs has been carried out implementing the capability for the GC column to run a temperature gradient, which can be exploited for increased compound separation.

The Scout3 system acts as a benchmarking instrument on the project for the SSP results and also can be configured to easily incorporate some of the developing sensor technologies if that is considered relevant.



Scout3 instrument, <https://volatile.ai/scout3>

Figure 2-2: Volatile Technologies

2.3 Description of UWAR system

UWAR is developing an electronics nose system consisting of a micro gas chromatograph (μ -GC), solidly mounted resonator (SMR) sensors and readout electronics. A version of the system with commercially available sensors is shown in Figure 2-6.

2.3.1 UWAR micro-GC progress summary

- ✓ Successfully developed a 2D spiral shaped micro-GC column model in COMSOL Multiphysics software.
- ✓ Printed a new micro-GC column with ceramic particle-based UV resin for improved thermal stability (stable up to 200 °C).
- ✓ Developed a method for uniform OV-1(PDMS) coating throughout the microchannel surface.
- ✓ Successfully tested three target VOCs: linalool, trans-2-hexenal, and ethanol.
- ✓ Conducted VOC testing at two different concentrations in both dry and wet air.
- ✓ Collected response data before and after column for processing, features extraction, and trained/tested a partial least square (PLS) model.
- ✓ Micro-GC work has been presented and accepted to present at three international conferences, Eurosensors 2024, IMCS 2025, Eurosensors 2025, UWAR is also preparing a draft for an IEEE journal publication.
- ✓ **Future Work:** UWAR is developing a new test rig to test lower concentrations (PPB level) of target VOCs.

2.3.2 Micro-GC modelling and simulation work

UWAR developed a 2D COMSOL Multiphysics model combining fluid flow and species transport to optimize Micro-GC column dimensions and stationary phase (SP) thickness. Four models with constant channel width (0.3 mm) were evaluated by varying channel length (l) and PDMS SP thickness (t):

- Model 1 ($l = 0.4$ m, $t = 10$ μ m),
- Model 2 ($l = 0.4$ m, $t = 3$ μ m),
- Model 3 ($l = 1.2$ m, $t = 10$ μ m), and
- Model 4 ($l = 1.2$ m, $t = 3$ μ m).

Column performance was assessed using the number of theoretical plates (N) and resolution (R_s), calculated from retention times. Model 4 showed the best performance with an R_s of 12 for ethanol and toluene. Results confirmed that longer channels and thinner SP layers improve separation efficiency. Figure 2-33 illustrates the 2D model, Figure 2-4(a) shows carrier gas velocity (average inlet velocity: 0.2 m/s), and Figure 2-4(b) presents species concentration profiles. Table 2-1 summarizes the performance metrics for all models.

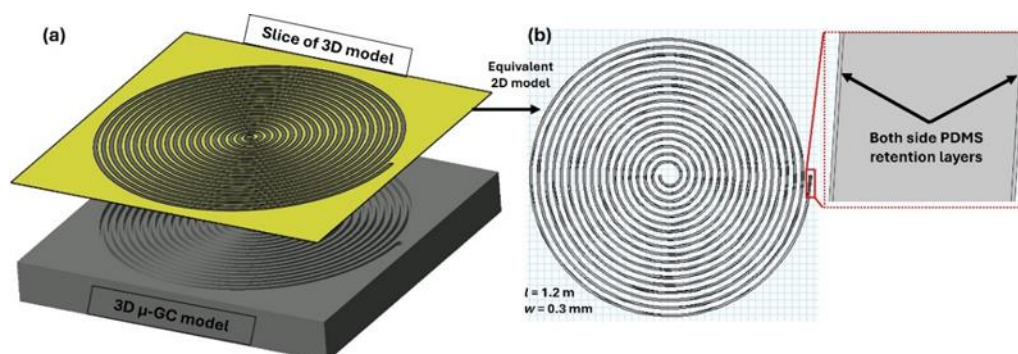


Figure 2-3: Developed μ -GC model in COMSOL for Multiphysics simulation.

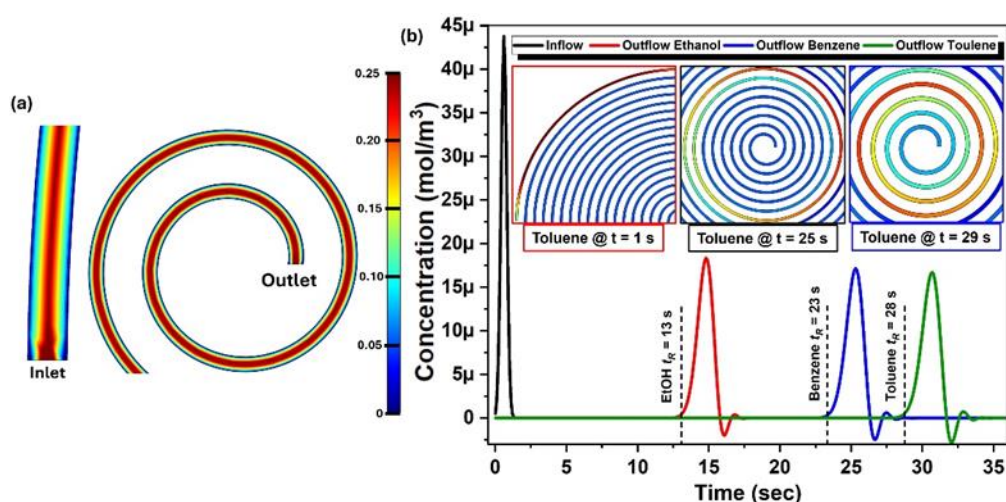


Figure 2-4: (a) carrier gas velocity profile, (b) model 4 inlet/outlet concentration profile; inset shows toluene profile at different time intervals.

Table 2-1: Performance comparison among simulated models.

Models	Species	N	R_S
1	Ethanol	62	
	Benzene	236	^a E/B=2.11
	Toluene	295	^b E/T=2.83; ^c B/T=0.8
2	Ethanol	178	
	Benzene	555	^a E/B=4.74
	Toluene	845	^b E/T=7.26; ^c B/T=2.48
3	Ethanol	197	
	Benzene	671	^a E/B=3.44
	Toluene	798	^b E/T=4.34; ^c B/T=1
4	Ethanol	650.77	
	Benzene	1735.68	^a E/B=8
	Toluene	2495	^b E/T=12; ^c B/T=4

^aethanol to benzene, ^bethanol to toluene, and ^cbenzene to toluene.

This work has been accepted to present in **IMCS 2025 conference** under the title of “**Design of low-cost 3D printed micro-gas chromatography (μ -GC) column for fast VOC analysis**”. The conference is scheduled to be held from 22nd - 26th June 2025 in Freiburg, Germany.

2.3.3 Design, fabrication, and testing of μ -GC columns

As reported in previous studies, a spiral-shaped Micro-GC column was designed in SolidWorks and fabricated using a low-cost 3D printer (Elegoo Mars 4 Ultra). Initially, the column was printed using Photocentric UV Basics HD Black resin. However, it was found that this resin's surface did not support uniform stationary phase (SP) deposition. To achieve a homogeneous OV-1 coating, the channel walls need to be functionalized with specific chemical groups, a process that typically requires temperatures around 200 °C. Since UV Basics HD Black resin degrades above 60 °C, it was unsuitable for this purpose. To address this limitation, Liqcreate Composite-X UV resin—capable of withstanding temperatures up to 200 °C—was selected. A new protocol was developed to functionalize the channel surface and enable uniform OV-1 coating. Figure 2-5 illustrates the Composite-X printed column, with Figure 2-5(a) showing the uncoated channel and its microscopic image, and Figure 2-5(b) displaying the OV-1-coated channel with corresponding microscopic imagery. A clear deposition of OV-1 coating can be seen in the microscopic images of the coating micro-GC column.

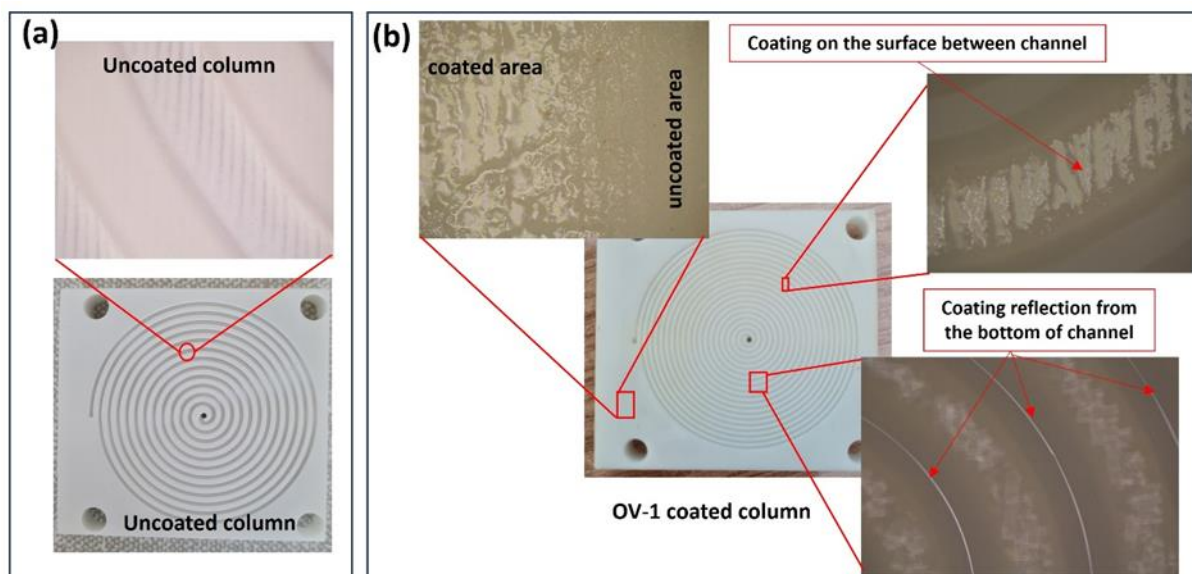


Figure 2-5: Composite x UV resin 3D printed column, (a) uncoated with a microscopic image, and (b) OV-1 coated column with microscopic images of different areas.

After successful coating, the column was integrated into the MOX-SMRs e-nose system, as shown in Figure 2-6. The complete MOX-SMR-GC-MOX-SMR unit was tested with target VOCs including ethanol, trans-2-hexenal, and linalool. As expected, ethanol eluted first, followed by trans-2-hexenal and then linalool. Tests were performed over multiple cycles at varying concentrations.

It was determined that the short 1.2 m GC column requires very low carrier gas flow rates (approximately 4–5 sccm) to ensure adequate retention times. However, the current setup only allows a minimum flow rate of 80 sccm, which remains too high. To address this, UWAR is in the process of installing a new test rig capable of achieving lower flow rates to enhance column performance.

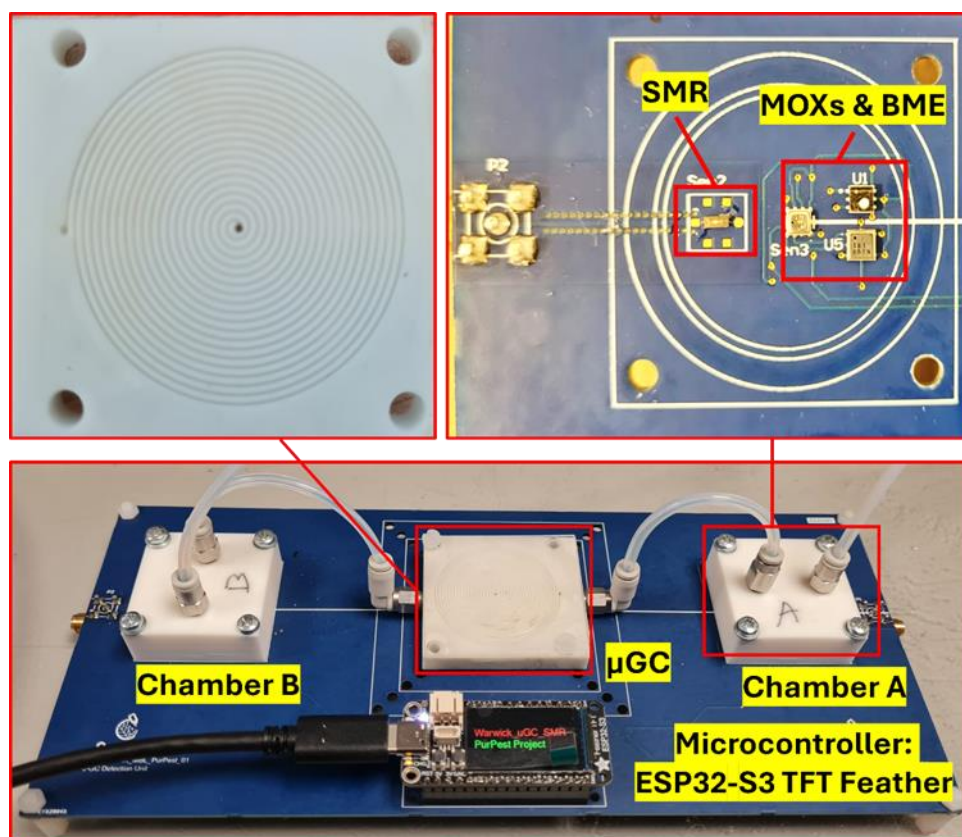


Figure 2-6: μ -GC based e-nose. Top shows μ -GC column, commercial MOX gas sensor and Bosch BME280 for ambient temperature and RH.

Figure 2-7(a) shows the response of the MOX sensor (before column) for all three VOCs, with an inset displaying a magnified view of the initial response curve of MOX to each VOC. The results demonstrate that MOX responds to all three VOCs simultaneously, but with varying curve slopes depending on the concentration and molecular properties of the compound.

Figure 2-7(b) presents the response of MOX sensor (after column) response, revealing delays of 1 s and 2.5 s for trans-2-hexenal and linalool, respectively, compared to ethanol (see inset in Figure 2-7(b)). These delays were expected due to the differences in molecular size, with lighter molecules eluting first.

Moreover, features were extracted from the time-dependent sensor responses (e.g. change in resistance, response time) and used to train and test a PLS model for the prediction of VOC class and concentration levels. Figure 2-8 shows confusion matrix for the trained model showed 100% accuracy in predicting unknown ethanol, trans-2-hexenal, and linalool concentrations. Further investigations are needed to control more accurately the inlet velocities of the target VOCs and life of the columns.

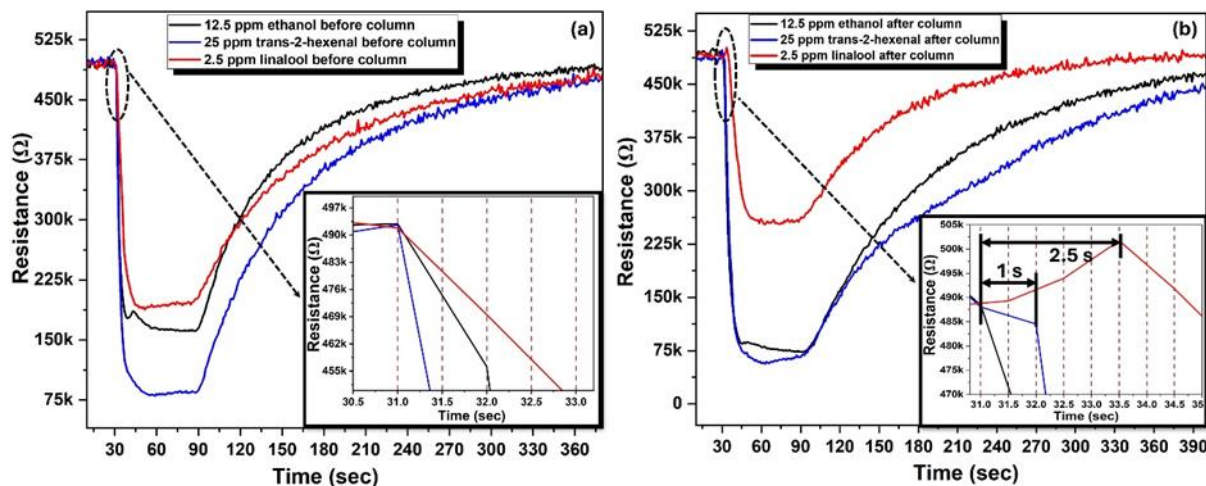


Figure 2-7: MOX sensors response, (a) before μ -GC, and (b) after μ -GC.

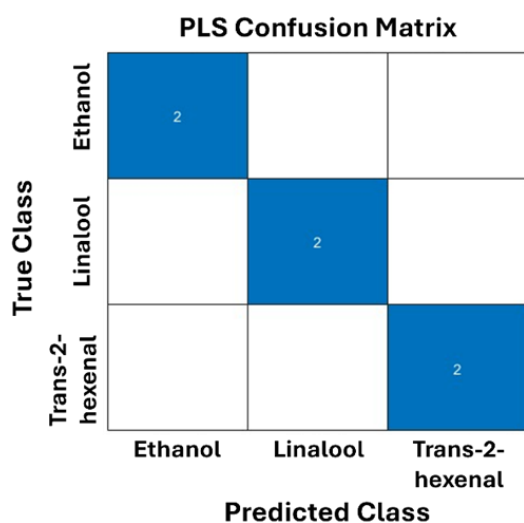


Figure 2-8: Confusion matrix for trained PLS model.

2.3.4 Publications to date on the micro-GC work

International conferences:

UWAR has reported and presented its work on the MOX-GC-MOX system at **Eurosenors 2024** [1]. The simulation-based research will be presented at the upcoming **IMCS Conference 2025** [2]. Furthermore, an improved version of the MOX-GC-MOX work has been accepted for presentation at **Eurosenors 2025** [3]. The titles of each work are listed below.

1. Usman Yaqoob, Siavash Esfahani, Marina Cole, Julian W. Gardner, "3D Printed Micro-Gas Chromatography (μ -GC) System for Improved Low-Cost VOC sensing.", Eurosenors 2024.
2. Usman Yaqoob, Siavash Esfahani, Marina Cole, Julian W. Gardner, "Design of low-cost 3D printed micro-gas chromatography (μ -GC) column for fast VOC analysis", IMCS 2025.
3. Usman Yaqoob, Dylan Limbani, Siavash Esfahani, Marina Cole, Julian W. Gardner, "3D-Printed μ -GC Integrated with an E-Nose System for Enhanced Plant Health Prediction" Eurosenors 2025.

Journal publications:

UWAR is working to collect data to draft a journal article on MOX-GC-MOX unit.

3 IMPROVEMENT OF THE INDIVIDUAL PARTS

3.1 Pre-concentration

The pre-concentration unit is described in detail in Deliverables D2.2 (*Report on Performance of Individual Sensor System Components – July 2024*) and D3.1 (*First Sensor System Prototype – September 2024*). It enables the pre-concentration and thermal desorption of target molecules emitted by pest-infested plants. This process significantly enhances the sensitivity of the gas chromatograph (GC) and allows detection at low parts-per-trillion (ppt) levels. No further work is required for this unit for the integration into the portable unit.

3.2 Separation

This section includes the improvement work done on the GC components by UWAR and AIRMO.

3.2.1 3D-printed μ -GC

3.2.1.1 Improvements and current limitations in micro-GC

UWAR developed a new coating method to uniformly coat 3D-printed columns and evaluated the column's performance using a MOX-GC-MOX unit with three target VOCs: ethanol, trans-2-hexenal, and linalool. As expected, ethanol eluted first, followed by trans-2-hexenal and then linalool. Further improvements are needed to enhance trace detection of the target VOCs and to improve separation resolution, which may be achieved by optimizing the carrier gas flow rate.

UWAR has so far tested higher concentrations of target VOCs, including ethanol at 25 and 12.5 ppm, trans-2-hexenal at 50 and 25 ppm, and linalool at 5 and 2.5 ppm. In the upcoming phase UWAR will focus on testing lower concentrations of these VOCs under both dry and humid air conditions, utilizing UWAR's newly developed testing rig, which is optimized for lower flow rates to enhance VOC separation. Additionally, UWAR plans to gather larger datasets to further train and validate the AI model for improved accuracy in VOC prediction. Concurrently, data collection is underway from the SMRs integrated on the PCB alongside the MOX sensors.

3.2.1.2 Future simulation work

Building on the current 2D modelling results, UWAR plans to develop a fully 3D simulation model of the Micro-GC column using COMSOL Multiphysics. This advanced model will incorporate the optimized channel length and stationary phase (SP) thickness identified in the 2D study. The 3D model aims to provide a more comprehensive understanding of fluid dynamics and analyte behavior within the column. Additionally, the simulation will be extended to include VOCs identified by the PurPest system, enabling a more realistic evaluation of column performance under practical conditions. This effort will support further optimization and design of high-efficiency Micro-GC systems for targeted applications.

3.2.2 Miniature GC columns

While UWAR is developing a low cost and robust new type of columns, VOL and AIRMO are using commercially available chromatographic columns. Commercial columns offer several important advantages that make them particularly suitable for field applications.

First, commercially available columns are widely accessible and come in a broad range of specifications, including different lengths, internal diameters, and stationary phase chemistries. This modularity allows for the selection of the most appropriate column dimensions and stationary phase properties to match specific analytical requirements, optimizing separation performance for

complex volatile organic compound (VOC) mixtures. Another significant advantage is that many commercial columns are available in metallic formats, which provide enhanced mechanical resistance. This makes them particularly well-suited for integration into portable or field-deployable systems, where ruggedness and durability are key requirements.

During the first intercomparison campaign and the preliminary evaluation conducted in Switzerland, it became evident that column resolution is a critical factor in achieving meaningful analytical results. The VOC profiles emitted by infested and non-infested plants are often highly complex and feature overlapping compounds with similar retention times. In this context, coelution can significantly hinder compound identification and quantification, potentially leading to incorrect conclusions.

To address this challenge, it was determined that only columns with lengths of 20 meters or more are capable of providing sufficient separation for these complex VOC mixtures. Shorter columns, although faster and easier to handle, do not offer the necessary resolution to distinguish between closely eluting compounds. Furthermore, both isothermal and temperature gradient configurations were tested: isothermal for the first SSP and gradient for the rack mounted system. The results clearly showed that isothermal operation fails to provide adequate separation for the full range of VOCs under study. In contrast, gradient temperature enables better peak separation across a broader volatility range, making it the only viable configuration for achieving good chromatographic resolution in this context.

In summary, the columns currently under development by UWAR, while very promising in terms of cost and mechanical durability, do not yet offer the resolution and separation efficiency required for reliable detection of VOCs in the PurPest context. As a result, commercially available columns have been selected for use in the next prototype which will be used in WP4.

3.3 Coating development for SERS and SMR

3.3.1 Introduction

The sensitivity and selectivity of the sensors developed in PurPest can be increased by orders of magnitude by choosing the most appropriate coatings that are both selective and sensitive to the target VOCs. This chapter describes the progress made in coating development.

3.3.2 Surface Metal-Organic Frameworks (SURMOFs)

Metal Organic Frameworks (MOFs) are permanently porous, regular 3D structures prepared from inorganic and organic building blocks. The wide range of available building blocks makes it possible to envision and prepare a vast number of MOFs. Due to both their fundamental properties and their potential applications, MOFs have received a significant amount of attention over the last decades. MOFs are commonly prepared as powders, and their properties have been studied and exploited in numerous areas.

When the term metal-organic framework was introduced, so was the acronym MOF. Authors from various institutions have chosen to name the material after the institution where it was first prepared, e.g., HKUST-1 (Hong Kong University of Science and Technology), UiO-67 (University of Oslo), and NU-1000 (Northwestern University), whereas others have categorized MOFs as coordination polymers and used the acronym CPO (Coordination polymer), e.g., CPO-27. To complicate matters even further, CPO-27 is the same material as MOF-74.

There are application areas where MOFs must be grown on the surface of a substrate and cannot be deposited as a powder, and the term Surface Metal Organic Frameworks (SURMOFS) is used to explicitly distinguish surface grown MOFs from powder deposited material. In PurPest we will

be concerned with SURMOFs, and they will be referred to as acronym@substrate to describe the MOF and the substrate it was grown on, e.g., HKUST-1@Au refers to HKUST-1 grown on Au. The simplified 2D sketch shown in Figure 3-1 illustrates the concept. Please note that the regularity extends in all three dimensions.

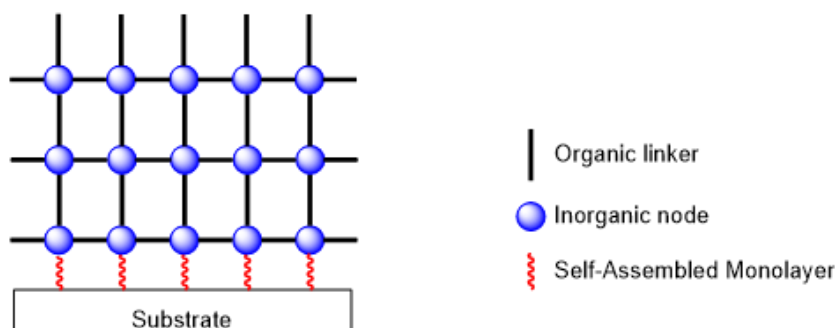


Figure 3-1: Simplified 2D sketch of a SURMOF. The structure extends in 3D.

SURMOFs can be prepared layer-by-layer on a surface. A self-assembled monolayer (SAM) on the substrate surface ensures adhesion between the substrate and first MOF layer. Exposing the surface to the inorganic and organic building blocks in an alternating fashion yields a well-defined SURMOF grown on the substrate. The self-limiting nature of the reactions and washing between layering with organic and inorganic building blocks are important to achieve the monolayers sketched in Figure 3-2. Since PurPest requires well-defined surfaces, the layer-by-layer preparation of SURMOFs is considered to be superior to other possible methods.

Some selected key issues addressed in PurPest are:

1. Identify the most suitable SURMOF for our purpose
2. Identify a suitable SAM to achieve the required MOF-surface interaction

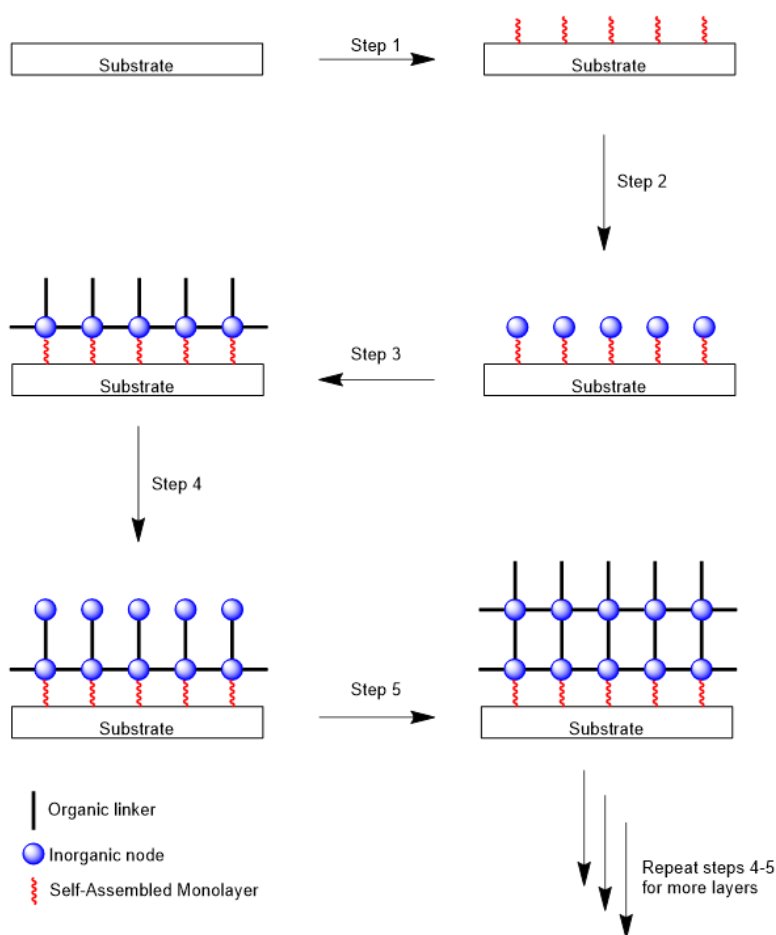


Figure 3-2: Sketch of layer-by-layer preparation of SURMOFs. Step 1: Self Assembled Monolayer (SAM) on substrate, step 2: first inorganic node deposition, step 3: first organic linker deposition, step 4: inorganic node, step 5: organic linker. The film thickness is controlled by repeating steps 4-5.

3.3.2.1 Experimental procedures

Commercially available starting materials and solvents were obtained from Sigma-Aldrich and Merck. All chemicals were used as received, and manipulations were carried out in the open air. HKUST-1 and MOF-177 were commercially available as powders, whereas all other MOFs were prepared according to literature procedures.

Si dies with a thin Au layer were prepared at SINTEF MiNaLab. The dies were rinsed with acetone in an ultrasonic bath for five minutes and then dried before use.

Spin coating

We first attempted to deposit MOFs on substrates by spin coating. Various MOFs and spin coating parameters were explored.

- Spin rates, and acceleration
- Deposited amounts of dispersion
- Viscosity of the dispersion media

Robotic dip coating (layer-by-layer deposition)

Slight modifications of a low-cost 3D printer provided us with a robot dip coater (Figure 3-3). The 3D printer head can move along the x,y,z -axes, thus, by placing solutions containing beakers in defined positions and moving the substrate from one beaker to another, layer-by-layer

deposition of the SURMOF was possible. Heat was provided by cartridges inside an Al-block placed on the 3D printer table. In the first generation of our set-up, we had to manually monitor the solution level and refill it when needed. In later generations we used lids to cover the solutions and minimize solvent evaporation.

After SAM deposition, samples were placed on custom made holders, and the holders were refined several times. It was important to make sure that the sample surface was exposed to the solution, the sample was stable on the holder the whole time, and a minimum of solvent and reactants was transferred between the various liquid reservoirs. The following steps 1-4 constitute one cycle:

1. Dip in solution containing inorganic building blocks
2. Wash
3. Dip in solution containing organic linker
4. Wash

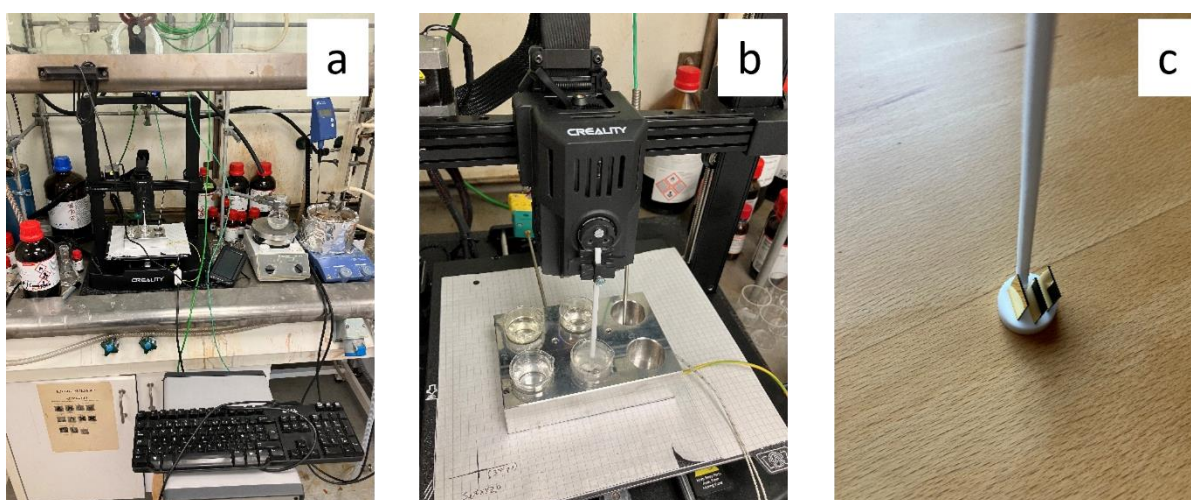


Figure 3-3: a, b: Robot for dip coating, c: Holder for dies (1st generation).

HKUST-1@Au

Self-assembled monolayer Au coated dies were rinsed in acetone on an ultrasonic bath for five minutes, dried, and placed in a solution of 4-mercaptobenzoic acid (4.7 mg, 3.1×10^{-5} mol) dissolved in ethanol (100 ml) at room temperature overnight.

$\text{Cu}(\text{OAc})_2$ $\text{Cu}(\text{OAc})_2$ (5.30 mg, 2.9×10^{-4} mol) was dissolved in ethanol (250 ml).

Linker $\text{H}_3(\text{btc})$ (1.38 mg, 6.56×10^{-5} mol) was dissolved in ethanol (250 ml).

Layer-by-layer deposition

Dip coating was carried out using the dip coater robot described above. At room temperature, SAM coated Au dies were placed in the sample holder and treated according to the following steps:

1. Cu(OAc)₂ solution for 15 min
 2. Ethanol for 5 minutes
 3. H₃(btc) solution for 15 min
 4. Ethanol for 5 min.
 5. Ethanol for 5 min
 6. Dry at 60 °C.
- ← Cycle

To avoid contamination, different ethanol baths were used in steps 2 and 4. Steps 1-4 are referred to as one cycle.

3.3.2.2 Characterization

Fourier infrared spectroscopy (FTIR) was carried out on a Bruker Vertex 70 equipped with a DTGS detector. The spectra were obtained from the SURMOFs were collected in reflectance mode. Each spectrum is the average of 16 scans at 4 cm⁻¹ resolution, unless otherwise noted.

Angle resolved X-ray photoelectron spectroscopy (AR-XPS) was performed on a *Thermo Scientific Thetaprobe* spectrometer using monochromatic Al K α radiation ($h\nu = 1486.6$ eV) and with an analysis area of approximately 400 μm diameter. Surface layer reconstruction based on the minimum entropy method was done using Thermo Scientific Avantage software.

Scanning electron microscopy (SEM) images, both based on secondary electrons (mostly topographic contrast) and back-scattered electrons (mostly atomic mass contrast), were obtained on a *FEI Nova NanoSEM650* field emission SEM. Energy dispersive spectroscopy (EDS) analyses were obtained with an *Oxford Instruments X-Max50* spectrometer attached to the SEM instrument.

3.3.2.3 Results and Discussion

Two commercially available MOFs and six MOFs prepared in house were screened for spin coating on Au dies. An overview of the MOFs is given in Table 3-1, and dispersion agents are given in Table 3-3.

Table 3-2. MOFs screened for spin coating.

MOF	Supplier
HKUST-1	Sigma-Aldrich
MOF-177	Sigma-Aldrich
UTSA-16	Prepared in house
UiO-67	Prepared in house
NU-1000	Prepared in house
ZIF-9	Prepared in house
ZIF-12	Prepared in house
MOF-808	Prepared in house

Table 3-3. Dispersion agents screened for spin coating.

Name	Acronym	Supplier
Water (H ₂ O)	-	In house
Dimethylformamide (C ₃ H ₇ NO)	DMF	Sigma-Aldrich
Perfluorononane (n-C ₉ F ₂₀)	-	Sigma-Aldrich

Perfluorooctane (n-C ₈ F ₁₈)	-	Sigma-Aldrich
Propyleneglycolmonomethyletheracetate (C ₆ H ₁₂ O ₃)	PGMEA	Sigma-Aldrich
Triethylglycoldimethylether (C ₈ H ₁₈ O ₄)	TEGDME	Thermo Scientific

We tested several combinations of MOFs and dispersion agents, and the visually most promising ones are given in Table 3-4.

Table 3-4. Spin-coating and some comments

Dispersion agent	MOF	Comment
H ₂ O	HKUST-1, MOF-177	Very uneven deposition. Spin rate = 0 yields the best result.
DMF	HKUST-1, MOF-177	Better than H ₂ O, but hard to remove solvent from pores.
n-C ₉ F ₂₀	HKUST-1	Improved wetting. Best so far.

The presence of HKUST-1 on Al and Au dies after spin coating was confirmed by FTIR spectroscopy, and the spectra are shown in Figure 3-4.

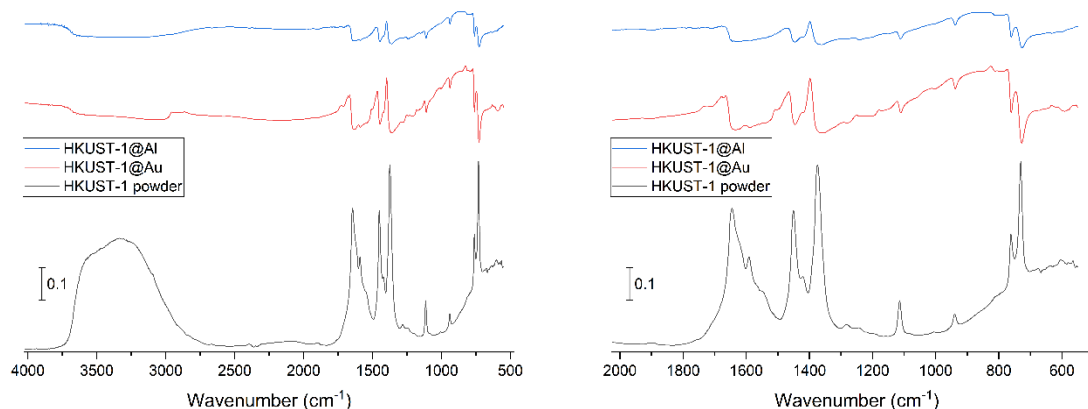


Figure 3-4. FTIR spectra of HKUST1-@Al and HKUST-1@Au prepared by spin coating of HKUST-1 dispersed in n-C₉H₂₀. The spectrum obtained from HKUST-1 powder is included for comparison.

The distribution of HKUST-1 on Al and Au is important in any application. Light microscopy showed that the MOF was non-uniformly distributed on both substrates, as shown in Figure 3-5. Figure 3-4

Figure 3-5 Furthermore, simple visual inspection revealed that spin coating did not deliver a reproducible deposition of HKUST-1. We conclude that, although spin coating and drop casting yield MOFs on surfaces, the quality is too low for our purpose.

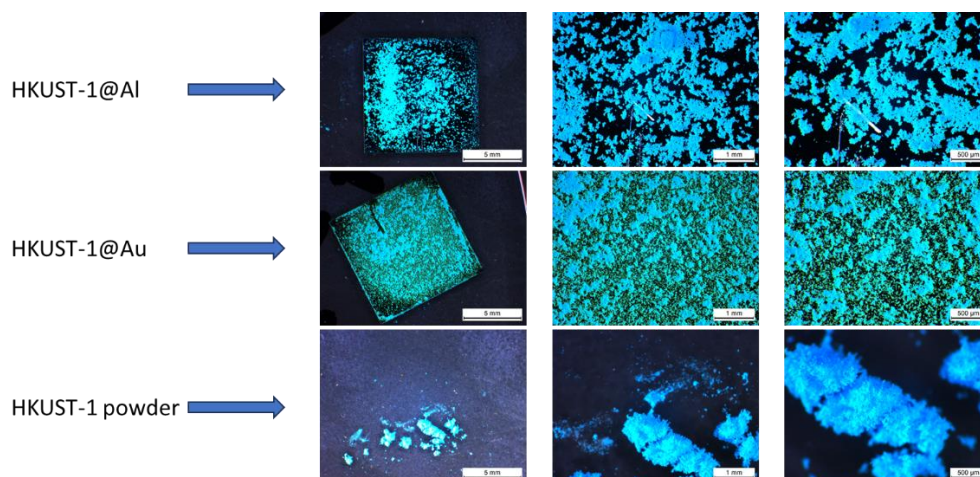


Figure 3-5. Light microscopy of HKUST-1@Al and HKUST-1@Au after spin coating a dispersion in n-C₉H₂₀. HKUST-1 powder is shown for comparison.

Interaction between MOFs and volatile organic compounds

FTIR was used to probe the interaction between HKUST-1 and ethanol, which is one of the volatile organic compounds (VOCs) of interest in PurPest. As seen in Figure 3-6, a band shift of 6 cm⁻¹ was observed upon exposure to ethanol. Thus, HKUST-1 is promising to be developed further as a part of a sensing device.

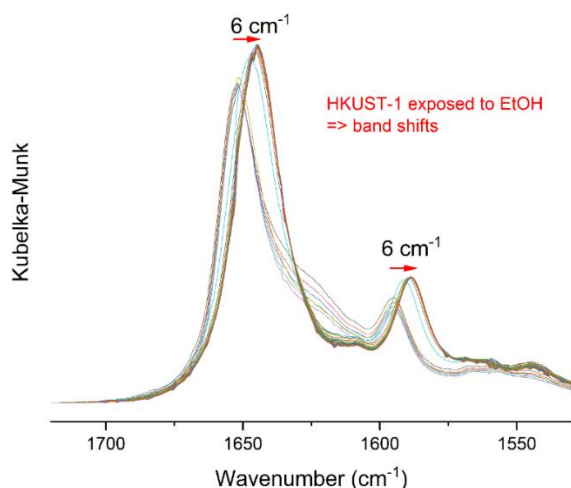


Figure 3-6. DRIFT spectrum collected from HKUST1 upon exposure to ethanol (EtOH).

Similar, promising observations were also made using Raman spectroscopy on UiO-67 during EtOH exposure.

SURMOFs prepared layer-by-layer (Dip coating)

Motivated by the promising FTIR and Raman studies on UiO-67, we first tried to prepare UiO-67@Au. After some time, we learned from the literature that UiO-67 SURMOFs require that the secondary building units (SBUs) are prepared separately, and this takes two weeks. In order to benchmark our set up and the newly built robotic dip coater, we decided to prepare HKUST1-@Au instead of UiO-67@Au. Once the system was benchmarked, we planned to return to the original plan of preparing UiO-67@Au if so desired. The presentation below does therefore not

reflect the project progress with time, as we find it more reader friendly to organize the section so that the science becomes clear.

HKUST-1@Au

Thiol SAMs on Au surfaces are well known. Our decision to use 4-mercaptobenzoic (**1**) acid as SAM is reasonable because of its resemblance to the carboxylate substituted aromatic fragment in the benzene-1,3,5-tricarboxylate (BTC) linker in HKUST-1. After SAM adsorption, layer-by-layer preparation was achieved by dipping the dies in $\text{Cu}(\text{OAc})_2$ and $\text{H}_3(\text{btc})$ solutions, respectively. The thickness, or number of layers, was controlled by the number of dipping cycles.

The preparation of HKUST-1@Au serves several purposes. HKUST-1 SURMOFs have been reported by others, thus, HKUST-1@Au can be used to benchmark the robot dip coater and our operating procedure. Once benchmarked, we will know that the expected challenges during the preparation of novel SURMOFs are mainly chemistry related. Furthermore, COMPAS aims to prepare SURMOFs on Si_3N_4 waveguides and it is therefore of interest to prepare HKUST-1@ Si_3N_4 . This will require another SAM than **1**, and benchmarking of the set up using established HKUST-1@Au is valuable. Our current hypothesis is that 4-vinyl benzoic acid (**2**) can be used as SAM on Si_3N_4 once surface -OH groups have been introduced on the surface of Si_3N_4 by exposure to HF.

Successful formation of HKUST-1@Au is supported by the FTIR spectra shown in Figure 3-7 and XPS spectra shown in Figure 3-9-8. The spectra collected from HKUST-1@Au compares well to the spectra obtained from commercially available HKUST-1 powder. The XPS results show that the SURMOF fully covers the surface, with no signal from Au detected (Figure 3-89). SEM images show a compact nanocrystalline layer with few defects on the surface, but with the additional presence of loosely attached agglomerates of nanoparticles (Figure 3-10). EDS analyses indicate that the nanoparticles are likely composed of HKUST-1 (not shown).

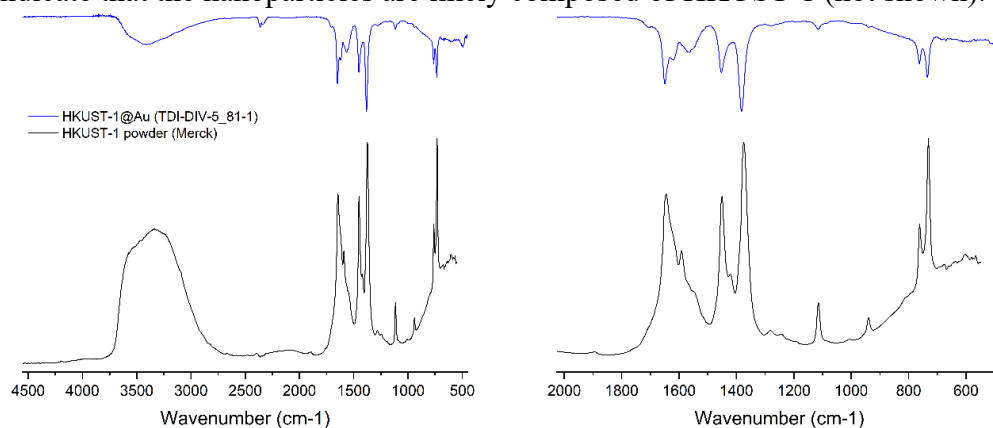


Figure 3-7. FTIR of HKUST-1@Au (upper, blue) compared to HKUST-1 powder (lower, black).

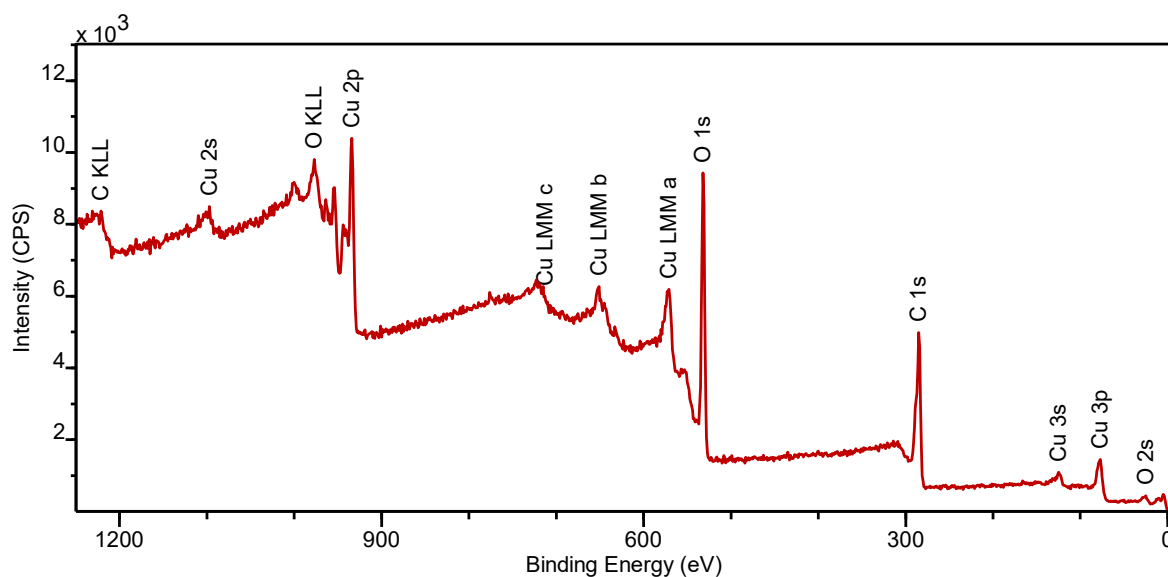


Figure 3-8. XPS spectra survey spectrum of HKUST-1@Au. Only the expected elements from HKUST-1 are detected (C, O, Cu; H cannot be detected), and the absence of Au signal confirms full coverage of the surface.

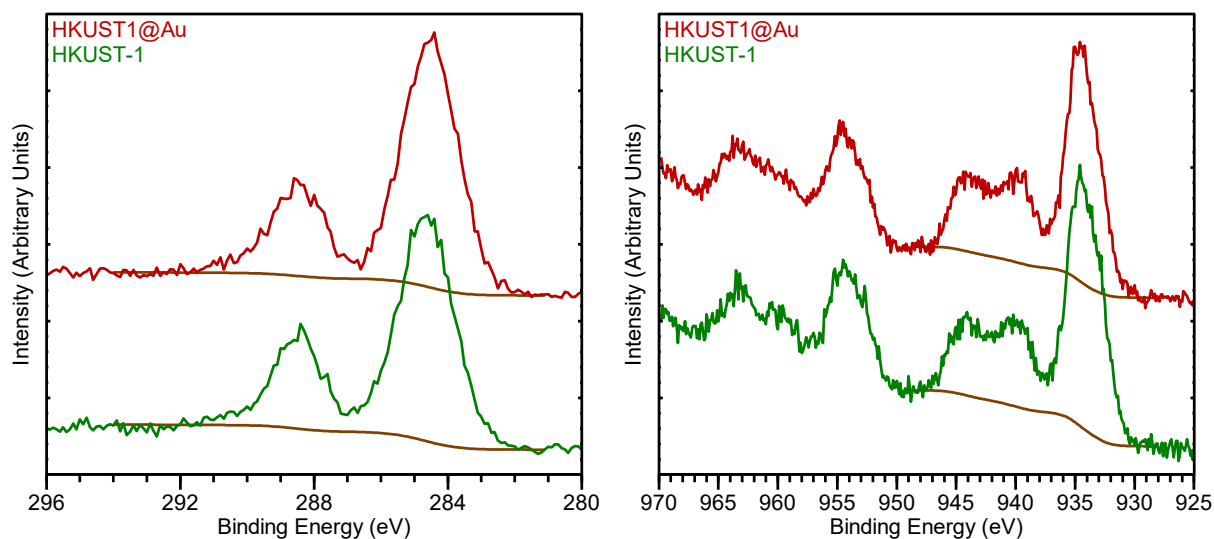


Figure 3-9. XPS detail spectra of (red) HKUST-1@Au and (green) commercial HKUST-1 powder. The (left) carbon 1s and (right) copper 2p energy regions are highly similar between the SURMOF layer and the reference powder, confirming highly similar chemistries.

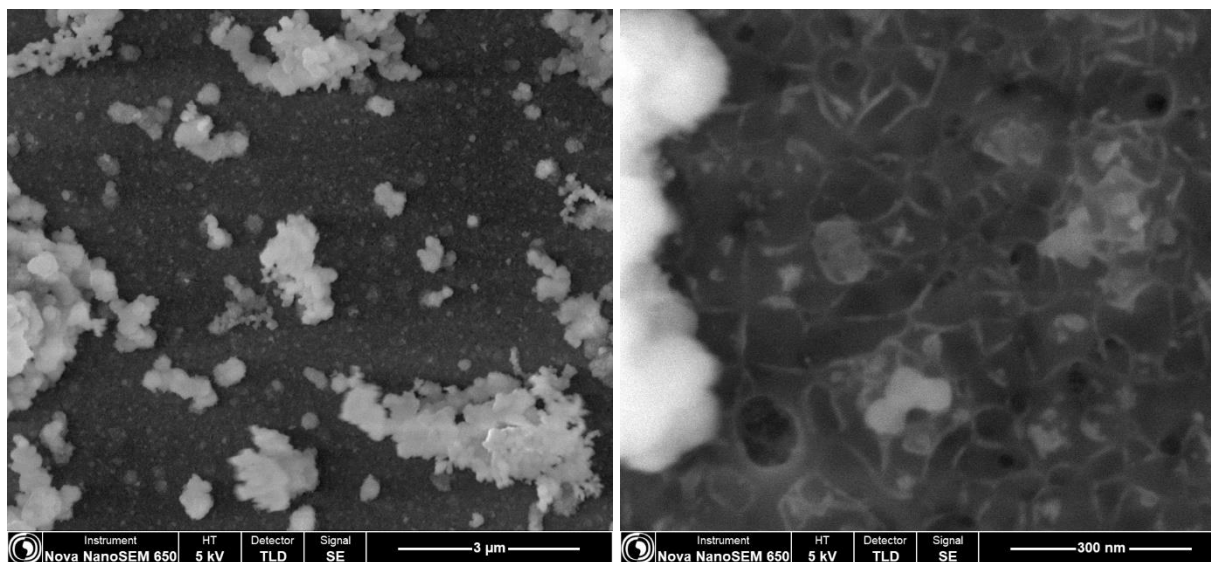


Figure 3-10. SEM images of HKUST-1@Au at two different magnifications, topographic contrast. A compact, nanogranular film with only few defects covers the sample surface, but with the additional presence of loosely attached agglomerates of nanoparticles.

On-going work

The UiO-series is interesting as sensing material due to the promising results obtained when we studied UiO-67 deposited on Au by spin coating. We are currently working on the deposition of both UiO-66-NH₂@Au and UiO-67@Au. We have successfully prepared UiO-66NH₂@Au by dip coating, but not yet documented its performance as a sensing layer, and we are currently working on UiO-67@Au. The results will be reported in due course.

3.3.3 UWAR coatings progress summary

- ✓ Four different coatings are prepared including ethyl cellulose, PDMS, rGO-SnO₂ and SnO₂ to target polar/non-polar compounds of the PurPest identified VOCs.
- ✓ UWAR and CMOS-compatible SMRs and commercial SMR provided by Sorex Sensors Ltd are prepared to coat with prepared coating materials.
- ✓ Four UWAR SMRs were coated with each prepared sensing material for reproducibility purposes
- ✓ Extra UWAR SMRs were also coated with each sensing material to place them in MOX-GC-MOX unit.
- ✓ Commercial Sorex SMRs are coated with the same coatings and tested for benchmarking the UWAR SMRs.
- ✓ **Future work:** UWAR is also planning to prepare some new coatings such as PEG, PEG-GO hybrid, and polyaniline (PANI) to coat them on the SMRs surfaces.

UWAR is actively advancing the development of specialized coating materials for use in VOC detection, specifically targeting the compounds identified by the PurPest project. Coatings based on ethyl cellulose and polydimethylsiloxane (PDMS) have been formulated to detect non-polar compounds such as d-limonene and linalool. For the detection of slightly polar to polar VOCs, such as trans-2-hexenal and ethanol, coatings utilizing reduced graphene oxide-tin oxide (rGO-SnO₂) and tin oxide (SnO₂) have been developed.

Following the recent identification of new plant-emitted VOC biomarkers associated with pest attacks by the PurPest team, UWAR has expanded its focus to include the development of

additional coating materials tailored to these newly identified compounds. The list of the compounds is presented in table 3-4.

Table 3-4 Volatile organic compounds produced by four target pests or their host plant after attack.

Pest	Plant	Partner	Ratio or single VOC	VOCs
FAW	N/A	UNINE	Single VOC	Phenol
FAW	Maize	UNINE	Single VOC	Indole
BMSB	N/A	UNIPD	Single VOC	Tridecane
BMSB	N/A	UNIPD	Single VOC	(E)-2-Decenal
CBW	N/A	NIBIO	Single VOC	1-dodecanol
PWN	Pinus pinaster	UEvora	Single VOC	2,4 dimethyl heptane
PWN	Pinus pinaster	UEvora	Single VOC	3-Penten-1-yne

Figure 3-11 presents optical microscopy images of SMRs coated with all prepared materials, including ethyl cellulose, PDMS, rGO-SnO₂, and SnO₂. The figure also includes the SMRs prepared for integration into the MOX-GC-MOX unit.

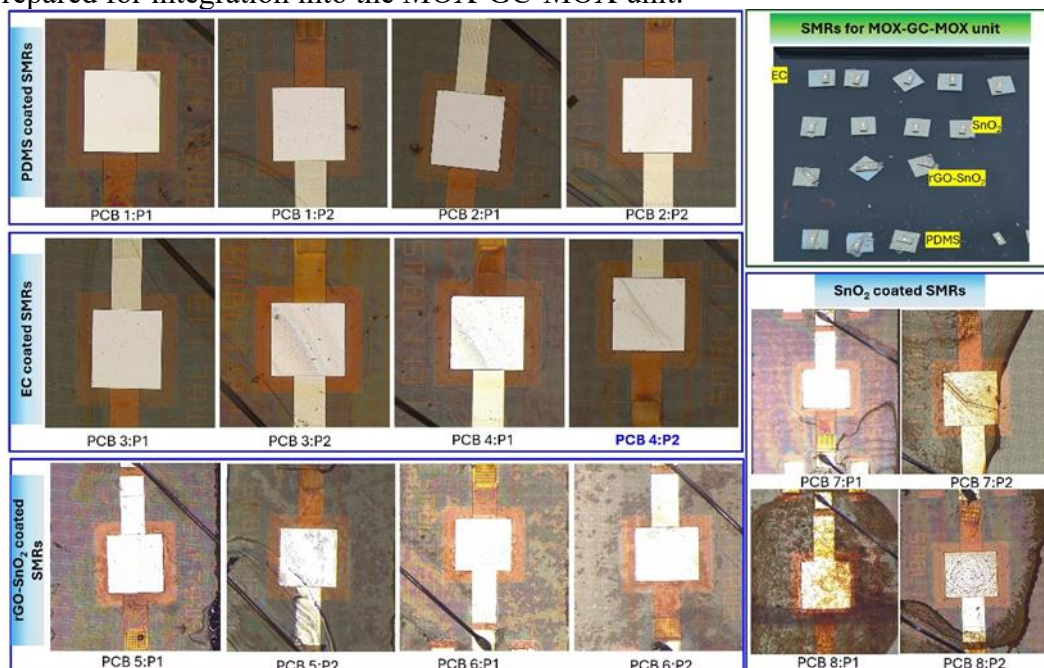


Figure 3-11: All SMRs are coated with prepared sensing materials.

3.4 VOC detection

3.4.1 Solidly mounted resonators

3.4.1.1 UWAR sensor progress summary

- ✓ A 3D printed dual chamber is designed and printed to facilitate the simultaneous detection of target VOC by both UWAR and commercially available Sorex Sensors Ltd. SMRs.
- ✓ Prepared SMRs are tested against the target VOCs.
- ✓ EC coated UWAR & Sorex SMRs shows a strong response to linalool at different concentration levels.
- ✓ A 1.5 m long heat exchange coil and a linear temperature compensation model are implemented to eliminate the effect of temperature on the sensor baseline.
- ✓ UWAR designed a new circuitry for SMR based e-nose system.
- ✓ UWAR has prepared a journal draft to submit the work in IEEE Sensors Journal, also UWAR work on SMRs, and linalool detection has been accepted to present in Eurosensors 2025.
- ✓ **Future work:** A clear plan has been developed to test all the coated SMRs with all target VOCs. UWAR will also coat more SMRs to detect newly identified VOCs.

3.4.1.2 Solidly mounted resonator (SMR) sensor development and coating evaluation

Solidly Mounted Resonators (SMRs) function by exciting a piezoelectric substrate within an oscillator circuit to generate a standing acoustic wave. The resonance frequency of this wave is highly sensitive to mass loading on the resonator surface, enabling the detection of volatile organic compounds (VOCs). Achieving high sensitivity and selectivity depends heavily on the choice of coating material applied to the resonator surface.

UWAR has developed a CMOS-compatible SMR device, which integrates a resonator, and a Bragg reflector fabricated using SilTerra Malaysia's standard 180 nm CMOS-MEMS/BAW process. This approach supports cost-effective fabrication and system-level integration; however, it results in a lower resonator quality factor (Q) due to a non-optimized Bragg reflector design. Figure 3-12(a) shows the CMOS compatible layer stack structure of the UWAR SMR [4]-[5].

To establish performance benchmarks, UWAR is also testing commercial SMRs supplied by Sorex Sensors Ltd. These devices are produced using a non-CMOS-compatible process, allowing for a more refined Bragg reflector design and consequently achieving a significantly higher Q factor.

Both UWAR and Sorex SMRs have been coated with various materials targeting specific VOCs, including ethyl cellulose, PDMS, rGO-SnO₂, and SnO₂. Ethyl cellulose-coated SMRs showed a particularly strong response to linalool. Additional test results for other coating and VOC combinations are presented in the following sections, along with a comparative table summarizing the performance of each SMR-coating configuration. The optical microscopic image of ethyl cellulose coated UWAR and Sorex SMRs is shown in Figure 3-12(b) and Figure 3-12(c).

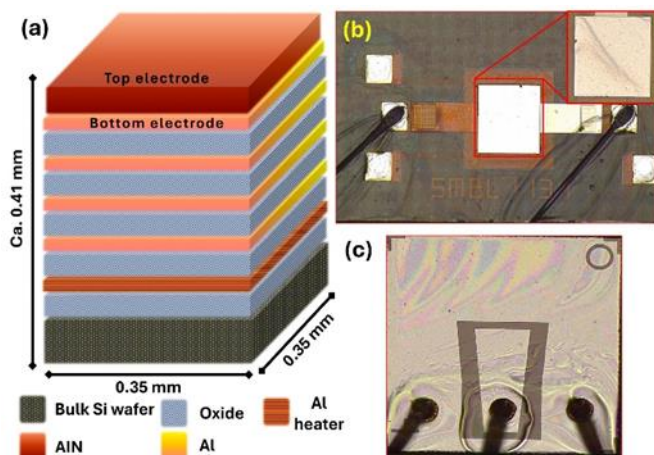


Figure 3-12: UWAR and Sorex SMRs, (a) CMOS compatible layer stack structure, (b) fabricated UWAR SMR coated with ethyl cellulose (EC), and (c) Sorex SMR coated with EC.

3.4.1.3 Design and integration of dual-sensor chamber for SMR based linalool detection

To enable simultaneous detection of linalool using both UWAR and Sorex SMR devices, a custom 3D-printed dual-chamber was designed and fabricated. This chamber allows the analyte to sequentially flow through both compartments, facilitating comparative sensing within a controlled environment. A BME280 environmental sensor was incorporated between the two chamber sections to continuously monitor ambient temperature and humidity during experimental runs.

The 3D-printed structure, shown in Figure 3-13, measures 10.5 cm in length, 5.0 cm in width, and 1.5 cm in height. Each SMR was housed in a dedicated, identically sized compartment with an internal diameter of 10 mm, a height of 6 mm, and an estimated internal surface area of 291 mm². Figure 3-13(b) and Figure 3-13(c) depict the custom-designed printed circuit boards (PCBs) developed for the UWAR and Sorex SMRs, respectively.

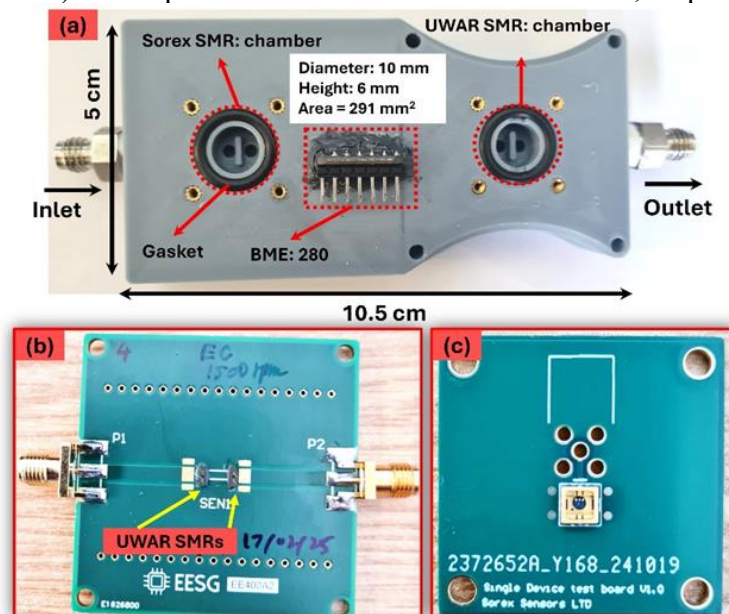


Figure 3-13:(a) 3D-printed dual-chamber with integrated commercial BME280 sensor, (b) PCB with UWAR SMR and, (c) PCB with packaged Sorex SMR.

To characterize the response of the SMRs to the VOCs, a fully automated mass flow control system was employed, controlled via a customized National Instruments LabVIEW program, the overall setup is shown in Figure 3-14.

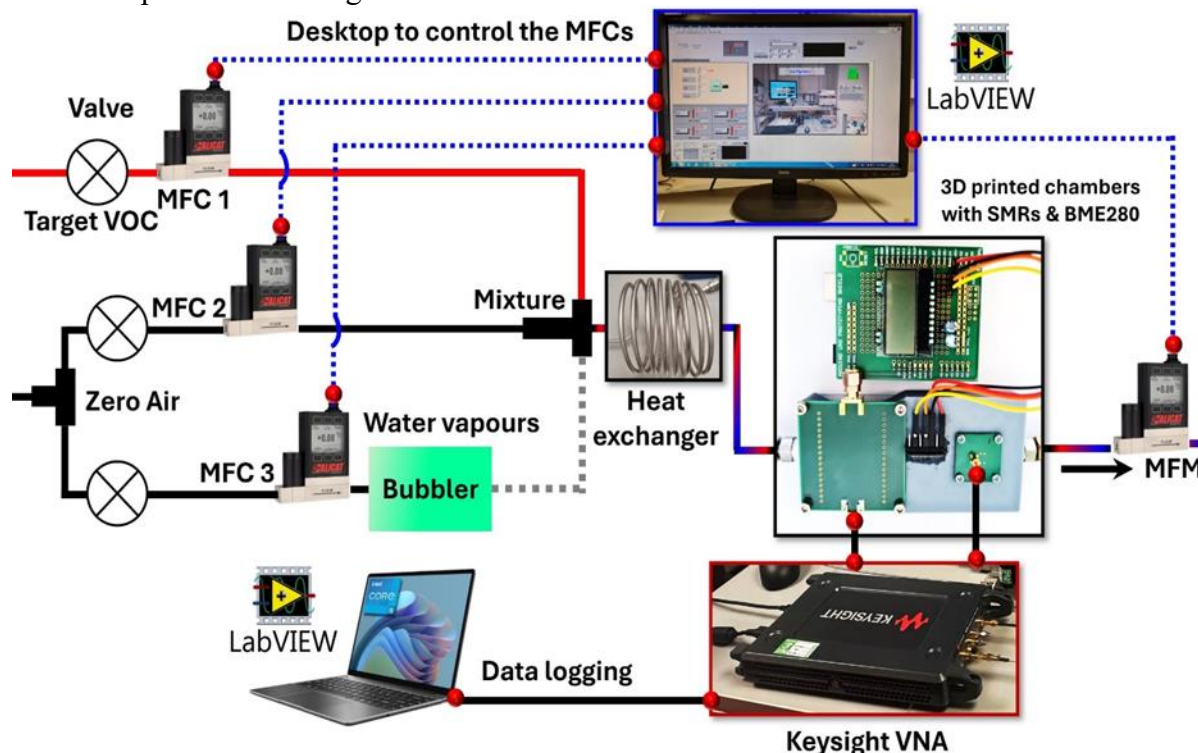


Figure 3-14: Experimental framework to evaluate SMR responses and document the data.

3.4.1.4 Results and discussions

To evaluate the sensing performance and reproducibility of the UWAR SMRs, three separate devices were prepared by spin-coating the ethyl cellulose (EC) solution under identical conditions. These devices were designated as S1, S2, and S3. The resonance spectra of each device before and after EC coating are shown in Figure 3-15(a)- (c). In all cases, a leftward shift in the resonance frequency was observed following EC deposition, indicating an increase in mass loading. Notably, sample S1 exhibited no significant change in attenuation, while S2 and S3 showed pronounced attenuation shifts. These differences are likely attributed to non-uniformities in the EC film thickness across devices, which affect both the resonance frequency and signal magnitude.

Figure 3-16(a) and (b) display the temperature-compensated responses, while the insets in each subplot illustrate the uncorrected raw data, with arrows indicating the direction of baseline drift, downward for the UWAR SMR and upward for the Sorex SMR. Both SMRs exhibited strong and rapid responses to linalool exposure. The UWAR SMR showed a sensitivity of 1.03 kHz/ppm, while the Sorex SMR demonstrated a significantly higher sensitivity of 15 kHz/ppm. To evaluate the influence of humidity on the sensing performance of both SMRs, measurements were conducted in an environment with 27% relative humidity (RH). Figure 3-17 presents the real-time, temperature-compensated responses of the EC-coated UWAR and Sorex SMRs to three concentrations of linalool (1, 5, and 7 ppm) under these humid conditions. The results indicate no significant deviation between responses in dry and humid environments, suggesting that the developed SMRs maintain stable performance under moderate humidity.

Moreover, the selectivity of the developed SMRs toward linalool was assessed by evaluating their responses to some other commonly emitted plant VOCs, specifically trans-2-hexenal and ethanol, at comparatively higher concentrations. Figure 3-18 presents a bar graph comparing the

cross-sensitivity of both UWAR and Sorex SMRs. Trans-2-hexenal was tested at concentrations of 80, 50, and 30 ppm, while ethanol was tested at 50, 40, and 25 ppm. In contrast, the sensors exhibited markedly stronger responses to linalool across all tested concentrations.

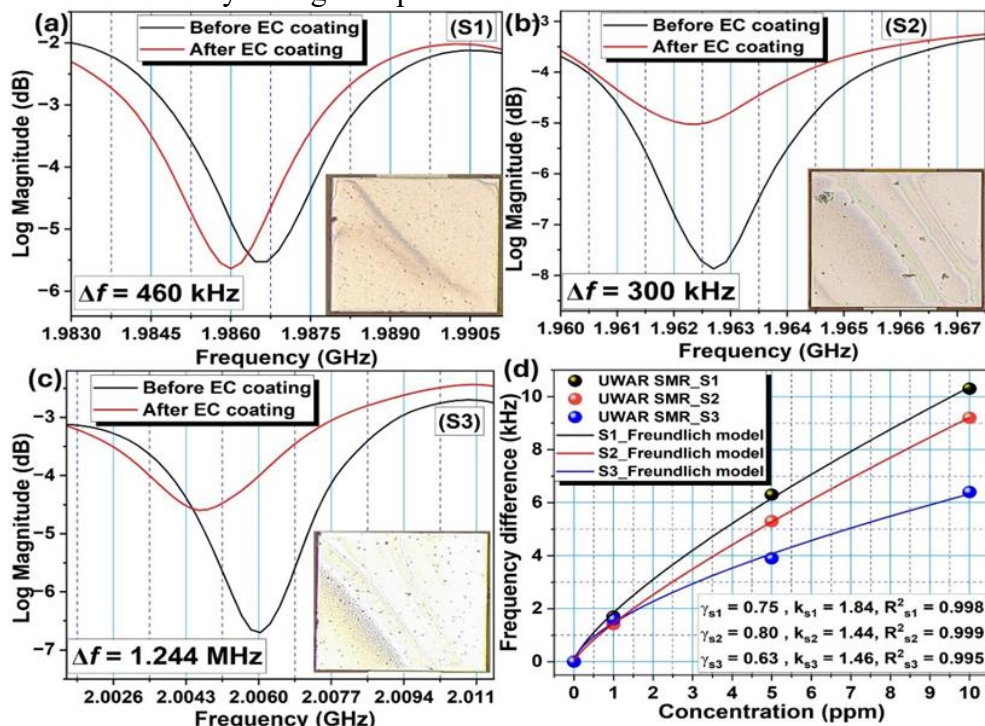


Figure 3-15 Figure 11. Resonance spectra of the three UWAR SMRs before and after EC coating: (a) S1, (b) S2, and (c) S3. Insets show the corresponding device surfaces with deposited EC film. (d) Frequency shift response of all three devices to 1, 5, and 10 ppm linalool, fitted with the Freundlich adsorption model.

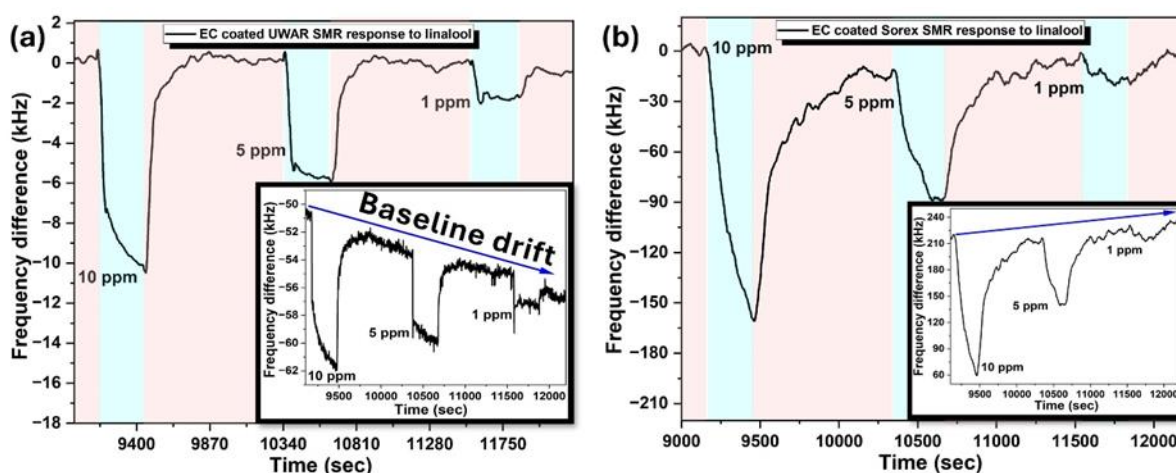


Figure 3-16 Figure 12. Temperature compensated frequency shift vs. time responses of SMRs to PPM levels of linalool in dry air environment (a) UWAR SMR, and (b) Sorex SMR, inset insets in each figure show the sensor responses before compensation, with arrows indicating the direction of baseline drift due to temperature fluctuations.

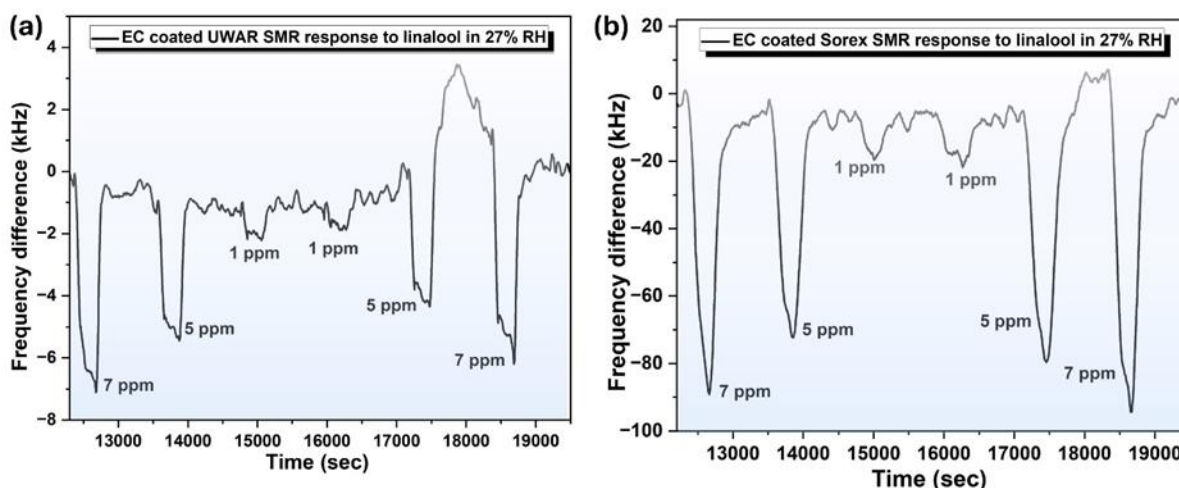


Figure 3-17: Figure 13. SMRs response to different concentrations of linalool in 27% RH (a) UWAR SMR and (b) Sorex SMR.

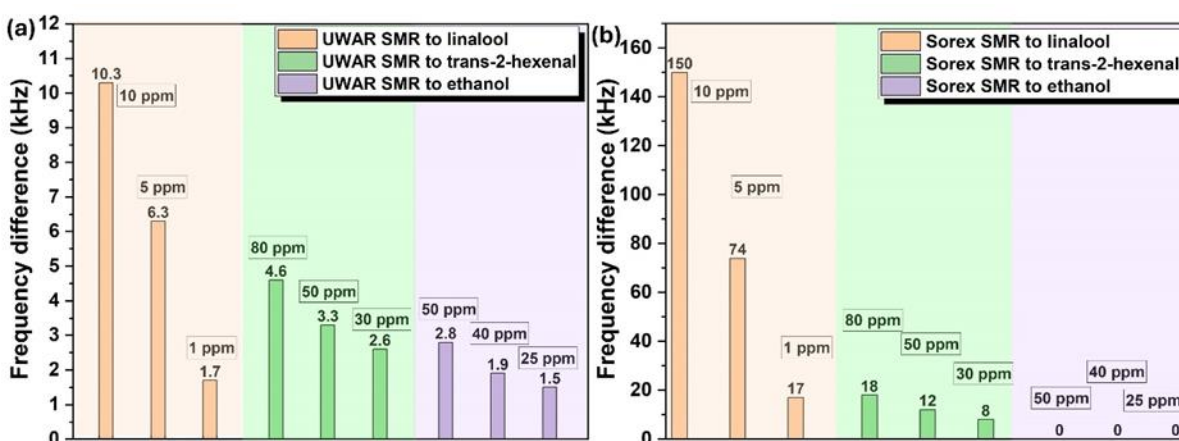


Figure 3-18: Figure 14. Cross sensitivity results (a) UWAR SMR, and (b) Sorex SMR.

3.4.1.5 Summary of SMR coating performance, sensitivity evaluation and future plan

As detailed in earlier sections, UWAR has developed and applied four distinct coating materials, ethyl cellulose, PDMS, rGO-SnO₂, and SnO₂, on both UWAR and Sorex SMR devices. These coated SMRs have undergone targeted VOC testing to assess their performance. The results of these evaluations, including the calculated sensitivity values for each SMR-VOC pairing, are presented in Table 3-5 and Table 3-6 below.

Moving forward, UWAR plans to complete the full set of tests under both dry and humid air conditions. Following this phase, the focus will shift to the characterization and detection of newly identified VOC biomarkers.

Table 3-5: Summary of UWAR SMR Performance with Various Coatings and Target VOCs

	Linalool		Trans-2-hexenal		Ethanol		D-limonene	
	Dry air	RH	Dry air	RH	Dry air	RH	Dry air	RH
	✓	✓	✓		✓			

Ethyl cellulose	S = 1.03 kHz/ppm	S = 0.99 kHz/ppm	S = 0.057 kHz/ppm	S = 0.056 kHz/ppm				
PDMS	✓		✓					
	S = 0.2 kHz/ppm		S = 0.023 kHz/ppm					
rGO-SnO ₂	✓		✓		✓	✓		
	S = 0.2 kHz/ppm		S = 0.051 kHz/ppm					
SnO ₂			✓					
			S = 0.035 kHz/ppm					

Table 3-6: Summary of Sorex SMR Performance with Various Coatings and Target VOCs

	Linalool		Trans-2-hexenal		Ethanol		D-limonene	
	Dry air	RH	Dry air	RH	Dry air	RH	Dry air	RH
Ethyl cellulose	✓	✓	✓		✓			
	S = 15 kHz/ppm	S = 12.75 kHz/ppm	S = 0.22 kHz/ppm		Nil			
PDMS	✓		✓					
	Nil		Nil					
rGO-SnO ₂	✓		✓		✓	✓		
	S = 27 kHz/ppm		S = 0.71 kHz/ppm					
SnO ₂			✓					
			Nil					

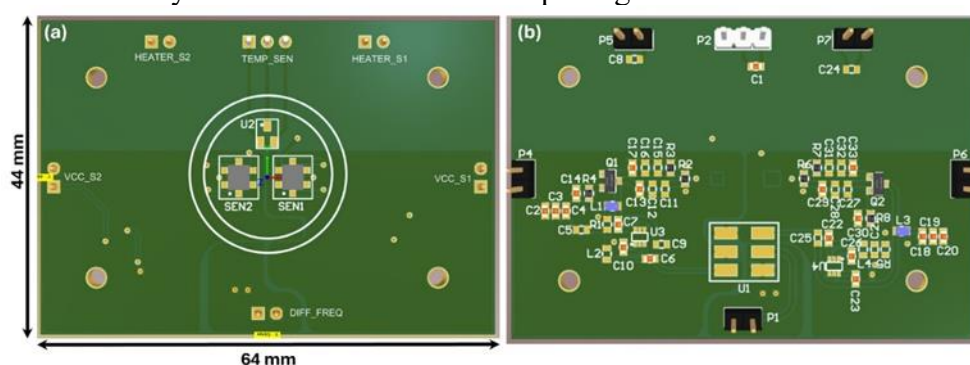
3.4.1.6 SMR e-nose progress

UWAR is currently refining the circuitry of its electronic nose (e-nose) system to resolve phase-locking issues previously observed among solidly mounted resonators (SMRs). To address this limitation, UWAR is implementing a revised architecture starting with a dual-SMR configuration comprising a functionalized (coated) SMR and an uncoated counterpart serving as a reference. Should this preliminary approach demonstrate effective phase de-correlation and signal stability, the system will be expanded into a full-scale e-nose array featuring four functional-reference SMR pairs.

In the updated design, each pair of SMR, comprising both the sensing and reference elements along with their respective oscillator circuits and a frequency mixer, are integrated onto a single printed circuit board (PCB). This PCB serves as a modular daughter board that can be inserted

into a centralized control board, enabling flexible operation of sensors with different coatings. By isolating all high-frequency components on the daughter board and transmitting only the resulting low-frequency mixer output to the control board, the design minimizes signal degradation and electromagnetic interference. The control board also supplies the required voltage rails for both the oscillator circuits and the SMR heater elements. A custom-designed, 3D-printed gas exposure chamber is mounted on top of the oscillator board to ensure consistent sampling conditions. The front and rear views of the SMR oscillator board are presented in Figure 3-19.

The second PCB acts as the central control unit and includes the microcontroller, signal conditioning filters, voltage regulation circuitry, and interfaces for low-frequency signal acquisition. Figure 3-20 and Figure 3-21 illustrate the front and rear views of the control board, as well as the fully assembled e-nose unit comprising both the oscillator and control boards.



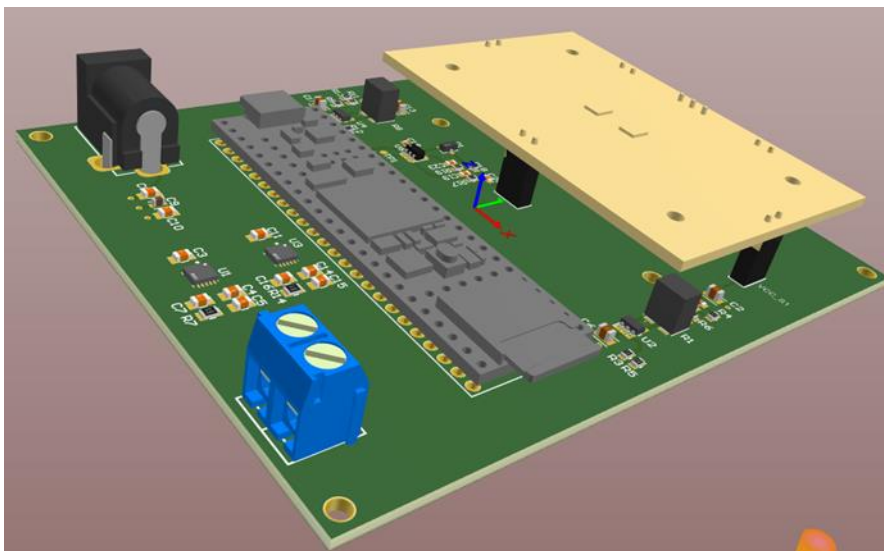


Figure 3-21: Figure 17: Assembled view of the SMR and microcontroller boards, showing the stacked configuration used for initial two-SMR testing.

3.4.1.7 Publications to date on the SMR-related work

International conference

UWAR recent work on SMRs has been accepted for a presentation at Eurosensors 2025 [6]. The title of the work is listed below.

1. Usman Yaqoob, Barbara Urasinska-Wojcik, Siavash Esfahani, Marina Cole, Julian W. Gardner, “Rapid Detection of Linalool Using Solidly Mounted Resonators for Plant Health Monitoring” Eurosensors 2025.

Journal publication

UWAR has drafted a manuscript reporting the EC coated SMR for linalool detection to be submitted in IEEE Sensors Journal [7].

1. Usman Yaqoob, Barbara Urasinska-Wojcik, Siavash Esfahani, Marina Cole, Julian W. Gardner, “Rapid and Selective Detection of Linalool Using SMRs for Plant Health Monitoring” IEEE Sensors Journal.

3.4.2 Photoionization Detector

3.4.2.1 Commercially available PIDs

A non-heated, commercially available photoionization detector (PID) was used as the detection unit in the first version of the sensor system prototype. The main advantages of this type of PID are its wide availability, low cost, and robustness. This detector was suited for the analysis of volatile and non-polar molecules. However, its performance was limited when detecting polar compounds such as D-limonene, which exhibited a very low response factor. To address this limitation, an initial modification of the detector was implemented, resulting in improved sensitivity, as described in Deliverable D3.1 (*First Sensor System Prototype – September 2024*). This modified detector was evaluated again during the inter-comparison at UNINE in March 2025. Because the detector remained unheated, the chromatographic peaks were broad, preventing reliable speciation of emissions from infested versus non-infested plants.

3.4.2.2 Heated PID prototype

Based on previous observations and considering the list of target molecules identified in WP1, a new heated PID was developed and manufactured. Most of the compounds identified as markers of pest-infested plants have boiling points above 150 °C, are polar, and occur at very low concentrations. To ensure effective detection, the sensor must therefore operate at temperatures exceeding 150 °C while maintaining sensitivity to both polar and non-polar molecules. This new detector was integrated into a rack-mounted system and evaluated during the March 2025 campaign (Figure 3-22).



Figure 3-22: Analytical systems used at UNINE for characterization of Fall Armyworm-Induced Volatiles in Maize

Over a two-week period, gas mixtures from both FAW-infested and non-infested maize plants were analyzed using two AIRMO gas chromatographs (including the newly developed PID) and a Proton-Transfer-Reaction Mass Spectrometer (PTR-MS) from UNINE as a referent system. Four different gas mixtures were prepared to evaluate the specificity and sensitivity of the analytical systems in characterizing Fall Armyworm (FAW) infestation in maize plants:

1. Glass vessel containing non-infested maize plant flushed with zero air
2. Glass vessel containing FAW infested maize plant flushed with zero air
3. Cage containing non-infested maize plants
4. Cage containing FAW infested maize plants

Gas mixtures obtained from experiments 1 and 2 enabled the analysis of FAW-induced volatiles in maize at ppb levels without interference from ambient air, as the glass bottles were flushed with zero air (air free of VOCs). In contrast, gas mixtures obtained from experiments 3 and 4 evaluated the performance of the analytical systems under more challenging conditions—at low ppt levels due to dilution of the volatiles in the room—and in the presence of potential interferent compounds from ambient air.

Under these conditions, all samples containing FAW-infested maize plants were successfully identified, thanks to narrow chromatographic peaks and strong signal responses across all target

compounds. Work is currently underway to develop the necessary electronics and integrate the improved detector into the portable unit, which will be evaluated in WP4.

3.4.3 SERS

3.4.3.1 Introduction

Surface-enhanced Raman scattering (SERS) is a very powerful and promising technique, since it allows for the “fingerprint” of specific molecules to be obtained without the need for labelling elements. The ability of SERS to detect extremely low concentrations of analytes leads to a wide range of applications in environment, industry and medicine. The signal enhancement in SERS relates to the excitation of localized surface plasmon resonances in metal nanoparticles (NPs). SERS is even capable of single molecule detection with signal enhancement factors up to 10^{15} .

SINTEF is developing SERS substrates for the detection of identified VOCs. The substrates are based on nanoparticles arrays, fabricated using nanoimprint technology (NIL), reactive ion etching (RIE) and thin film deposition. The shape and size of the nanoparticles are specifically designed to enhance the Raman signal from the selected VOCs. SAFTRA photonics has developed and patented a breakthrough "PickMolTM tailored/personalized nanotechnology" designed for the selective and highly sensitive detection of trace amounts of organic molecules in various matrixes (environment, pharmaceutical and food industry, medicine). In Purpest, SAFTRA Photonics is working on SERS system for VOCs detection.

3.4.3.2 Simulation and design

The simulations were conducted employing the Finite-Difference Time-Domain (FDTD) method, implemented in Ansys Lumerical commercial software. The model employed for simulation was a comprehensive 3D representation, incorporating substrates to enhance the accuracy of the simulation results (Figure 3-23 a). Specifically, the model included an array of nanostructures with a height of 200 nm and positioned on a silicon (Si) substrate. A selected number of nanostructures were included in a rectangular simulation volume, with the perfectly matched layer (PML) boundary conditions in the X direction (propagation direction) and periodic boundary conditions in the Y and Z direction. The PML and periodic boundary conditions were selected to minimize reflections and simulate an infinite array, respectively. The substrate was illuminated from the top by a broadband plane wave spanning the wavelength range of 500 to 1600 nm. The reflected intensity was measured above the substrate, while the electric field distribution was recorded at the gold-air interface. Different patterns were designed and simulated and 5 were selected and a lithography mask was designed where the designs are distributed over a 6” inch Master wafer (Figure 3-23 b).

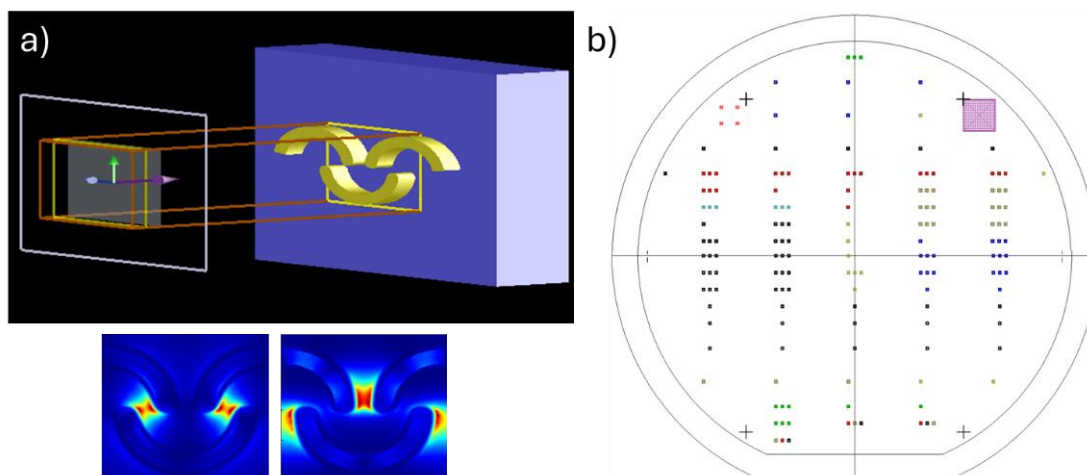


Figure 3-23 a) Simulation model – 3D visualization, the violet arrow shows the propagation direction and the electric field distribution; b) mask design, with SERS areas distribution for the UV-NIL Master

3.4.3.3 Fabrication

Two types of SERS substrates are used in the Purpest project:

- Designed nanopatterned arrays fabricated using UV-NIL.
- Random gold nanoparticles.

For the fabrication using UV-NIL, the designed Master wafer was ordered from NIL Technology (Denmark) and delivered in mid-May 2025. Current work focusses on optimizing the fabrication process in SINTEF cleanroom facility.

Fabrication process of substrates with random gold particles (N5)

A 6" silicon wafer was coated with gold, patterned using standard lithography and metal etching to create active areas and annealed in 400 °C for 30 min creating random distribution of gold particles Figure 3-24. Lastly, the substrates were coated with additional layer of gold, 20, 40, 60 and 80nm and enhancement of Raman signal was compared.

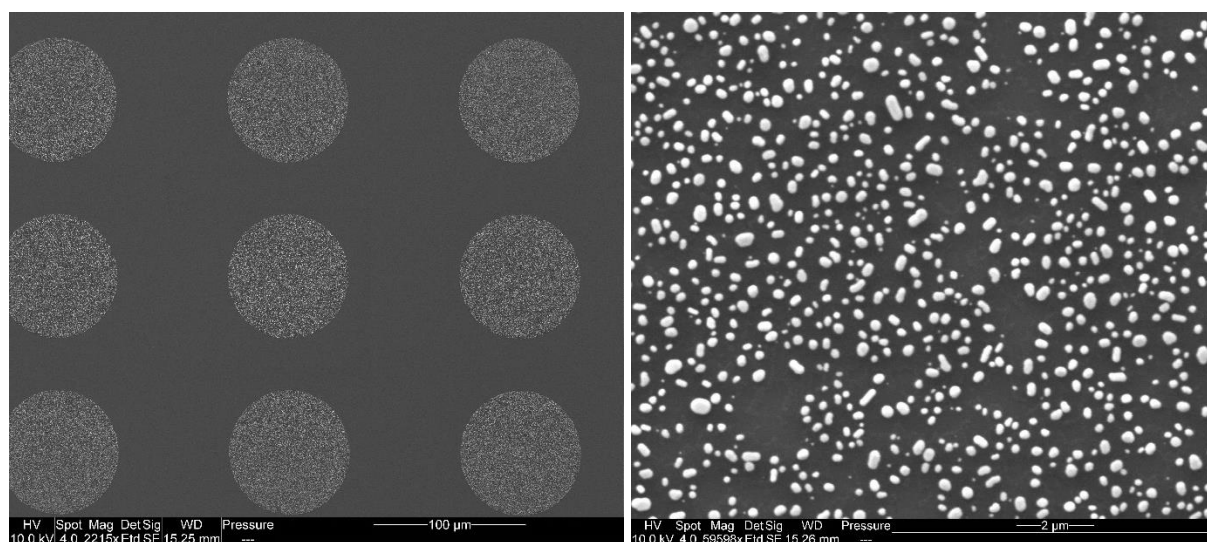


Figure 3-24 Scanning electron microscope (SEM) picture of the fabricated N5 substrates before additional coating of gold.

3.4.3.4 Measurements and results

The SERS measurements using N5 substrates gave good enhancement results (Figure 3-25). Current work focuses on coating the N5 substrates with MOFs for VOCs collection.

N5 substrate with HKUST-1

In Figure 3-25 one can see a comparison of the Raman spectra between HKUST-1 on blanket Au and on N5 substrates. Even with 50% of the laser power and 50% of the integration time, the N5 substrate gives about 2x the Raman signal intensity at the 1070 cm^{-1} peak, indicating a total enhancement of 8x (2^3).

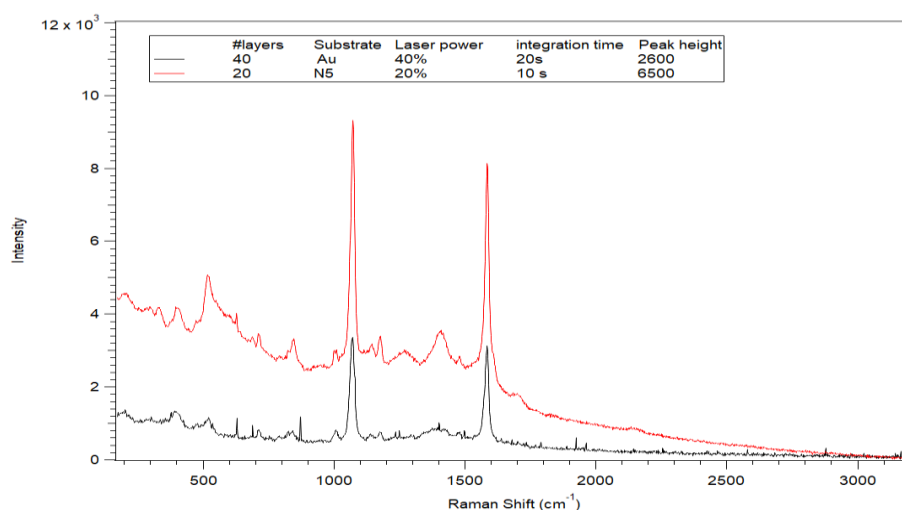


Figure 3-25: Comparison of the Raman spectra between HKUST-1 on blanket Au and on N5 substrates. Even with 50% of the laser power and 50% of the integration time, the N5 substrate gives about 2x the Raman signal intensity at the 1070 cm^{-1} peak.

N5 + HKUST-1 exposed to ethanol > 60 ppm

The N5 sample in Figure 3-26 was exposed ethanol during continuous measurement of the Raman spectra. Unfortunately, we did not observe any significant shifts in peaks or the appearance of new peaks. But as can be seen in Figure 3-26 there is a decrease in intensity of about 6% of the peak at 1585 cm^{-1} .

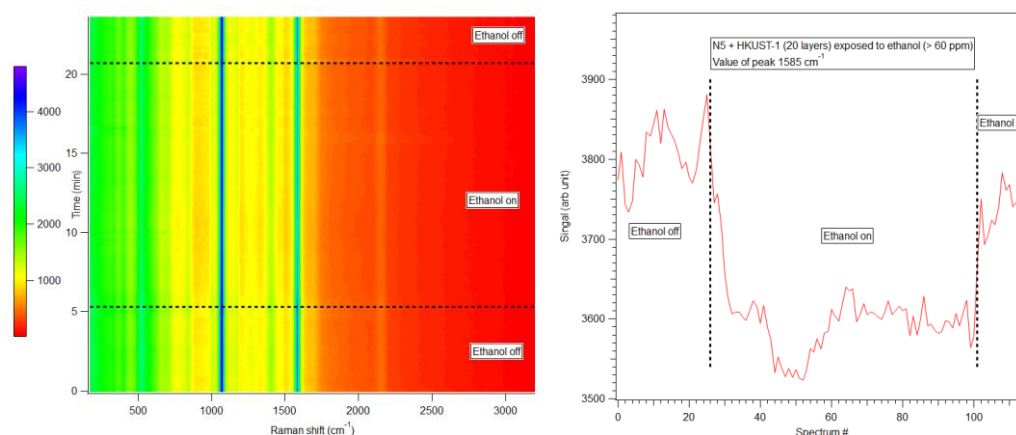


Figure 3-26: Left: 2D plot of signal intensity vs time and Raman shift with indications of when the sample was exposed to ethanol vapor at > 60 ppm. To observable shifts. Right:

intensity of the peak at 1585 cm^{-1} showed a slight decrease (approx. 6%) during ethanol exposure.

HKUST-1 on Au exposed to 2-methyl-1-butanol

The sample with HKUST-1 on blanket Au shown in **Error! Reference source not found.27** was exposed to 2-methyl-1-butanol for a prolonged period of time. To the left in Figure 3-27 one can observe some intensity peaks appearing in the Raman spectra at 1113 cm^{-1} and 1492 cm^{-1} during exposure to 2-methyl-1-butanol. To the right in the same figure these can be seen in the time domain. There is a clear increase in intensity during VOC exposure, and it relaxes after the VOC is turned off. This indicated that HKUST-1 was a potential MOF candidate for 2-methyl-1-butanol. However, we were not able to replicate these results in subsequent experiments.

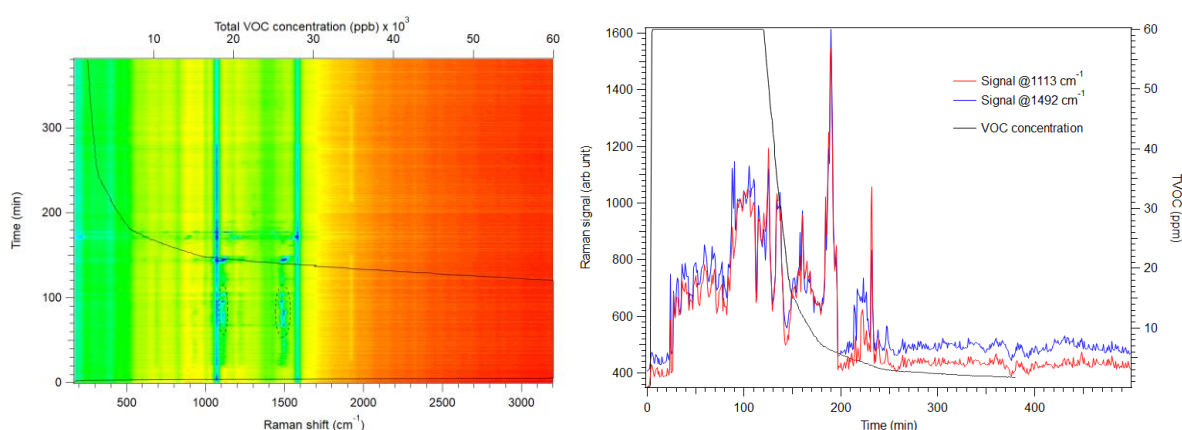


Figure 3-27: HKUST-1 on blanket Au exposed to 2-methyl-1-butanol. The left image indicates some peaks appearing at 1113 cm^{-1} and 1492 cm^{-1} . To the right one can see these peaks in the time domain. There is a clear difference in the signal between the time when the sample is exposed to ethanol and not.

UiO-67 powder on Au exposed to high concentration limonene

Pure UiO-67 powder was drop cast on Au surface and measured while being exposed to high concentrations of limonene. In Figure 3-28 one can see two peaks at 760 cm^{-1} and 1645 cm^{-1} that both showed significant change in intensity. In addition, the peak at initial 1421 cm^{-1} shifted to 1411 cm^{-1} .

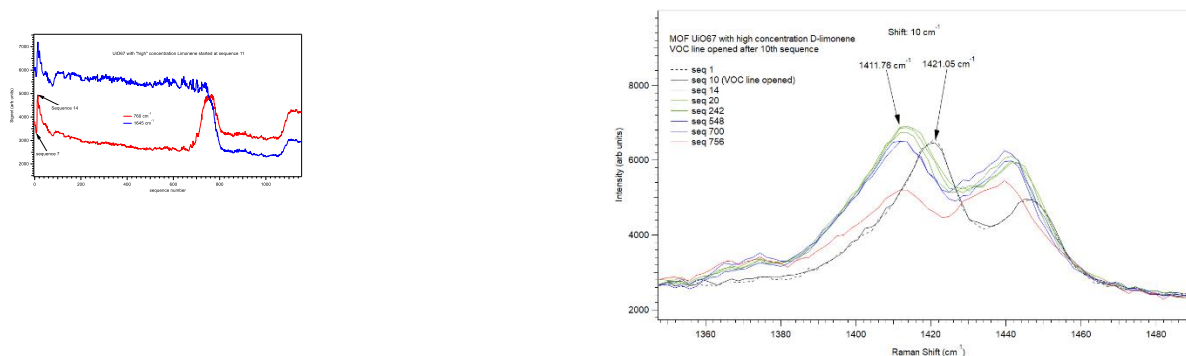


Figure 3-28: UiO-67 powder on Au surface exposed to high concentration limonene. The Two spectra are taken out since these seemed to indicate a response. Also, the peak at initial 1421 cm^{-1} shifted to 1411 cm^{-1} .

Other experiments

In addition to the experiments described above, SINTEF has done many more experiments on various MOFs on blanket Au and N5 with different VOCs. As of the writing of this report, we have not been able to identify a combination that can give us definitive good results.

Conclusion

SINTEF has tested multiple combinations of substrates, MOFs and VOCs. There were some early indications of potential candidates, but none have given repeatable and satisfactory results. The reason for this could be many, but one major one could be that due to unforeseen circumstances SINTEF has not been able to fabricate the SERS structures designed (see section 3.4.3.2) for the project. This is because the materials available for the NIL processes not being sufficiently CMOS compliant (too high levels of certain trace elements that are strictly prohibited in our laboratory due to detrimental effects it will have on other fabrication). However, SINTEF has now identified and qualified new materials that we can use for NIL and hence in Q3 2025 we will have several SERS chips for further testing.

3.4.4 PickMol technology

3.4.4.1 Introduction

Raman spectroscopy – a current area of research into improving the speed and accuracy of the identification of molecules in an environment including a clinical environment is using the phenomenon of the inelastic scattering of light, Raman scattering.

It has been shown in several studies that Raman microspectroscopy is capable of rapid identification of different organic and biological molecules. It is a powerful technique providing "fingerprints" of specific molecules without the need for labelling elements. However, Raman signal is very low and therefore requires enhancement for practical applications.

There are different approaches to increase the intensity of Raman signals, such as for example: resonance or nonlinear Raman spectroscopy. The problem is that these approaches/techniques in a big majority of cases need an expensive and sophisticated experimental set-up and thus, these techniques are not suitable for an on-line/on spot measurement. As was shown in many recent studies, Surface enhanced Raman scattering (SERS) could be such a method.

SERS has become a mature analytical technique that significantly increases the Raman scattering cross section. The ability of SERS to detect extremely low concentrations of analytes leads to a wide range of applications in the environment, industry, and medicine. The signal enhancement in SERS relates to the excitation of localized surface plasmon resonances in metal nanoparticles (NPs). SERS is even capable of single molecule detection with signal enhancement factors up to 10^{15} .

Plasmons are oscillations of electron plasma that are excited by light on metal nanoparticles; the excitation results in generating a significantly enhanced electromagnetic field (EMF) on the surface of the nanoparticles due to the localized surface plasmon resonance (LSPR). EMF is increased many orders in hot spots (HS) - The selectivity and sensitivity of the method can be significantly increased by a functionalization of NPs with a suitable linker/cavitands molecules with specifically bind of molecule of interest (analyte) (Figure 3-29)

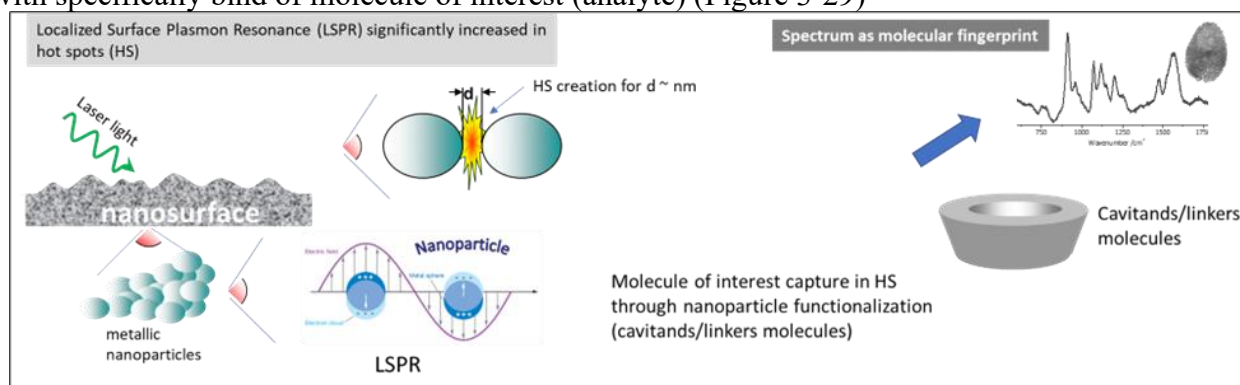


Figure 3-29: Physical principle of SERS spectroscopy and schema of surface functionalization

Recently, for various SERS applications, different sophisticated substrates are exploited such as metallic nanostructured surfaces, nanoantennas of different shapes, colloidal NPs, and clusters of metal spheres. SAFTRA photonics has developed and patented a breakthrough "PickMolTM tailored/personalized nanotechnology" designed for the selective and highly sensitive detection of trace amounts of organic molecules in various matrixes (environment, pharmaceutical and food industry, medicine). In Purpest, Saftra Photonics and SINTEF are working on developing surface-enhanced Raman spectroscopy (SERS) system for VOCs detection. The SERS sensing comprises three parts: the Raman spectrometer, flow cell, and SERS nanostructured chip.

3.4.4.2 Development and fabrication

To achieve the main goal of the PURPEST project – the detection of very low concentrations of VOCs can be divided into three related steps:

1. RAMASCOPE spectrometer was modified/tailored in its optical part (optimizing the trajectory of the excitation light for new “flow cell”) and mechanical part (optimizing the position of the flow cell holder). Moreover, PickMol software was developed for measuring VOCs (repeated measurements) – Figure 3-30

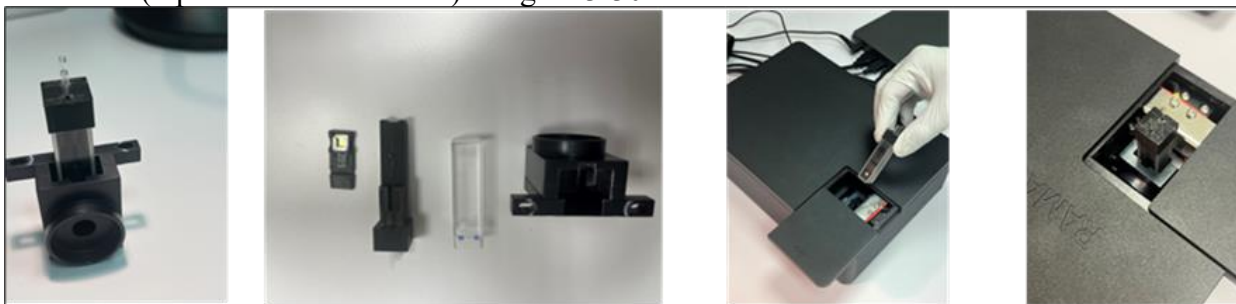


Figure 3-30: Sample holder and optical path modification of the RAMNASACOPE detection system

2. New “flow cel” assuring a laminar flow of air (containing volatile molecule of interest) has been developed - Figure 3-31.

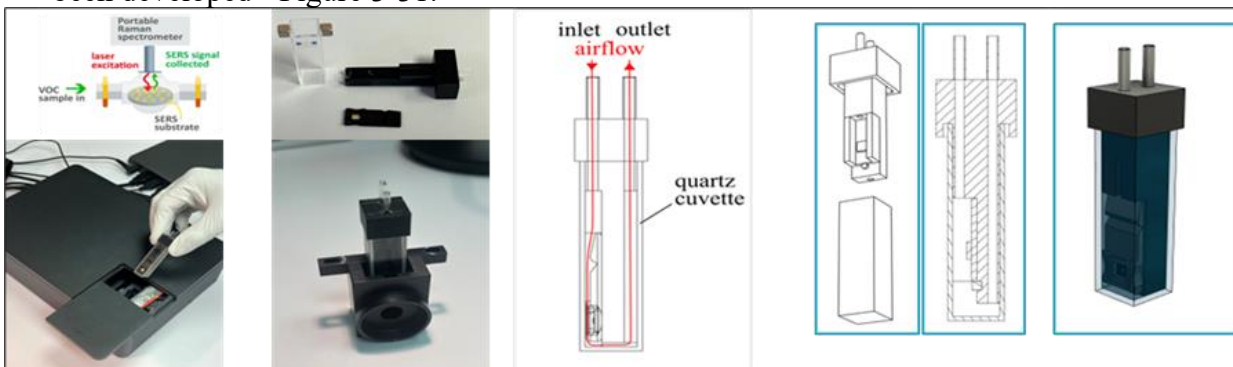


Figure 3-31: New design of “flow-cell and its position in the sample holder

A suitable experimental set-up consisting of: i) air pump, ii) sample box, iii) flow cell, iv) RAMASCOPE has been arranged – Figure 3-32.

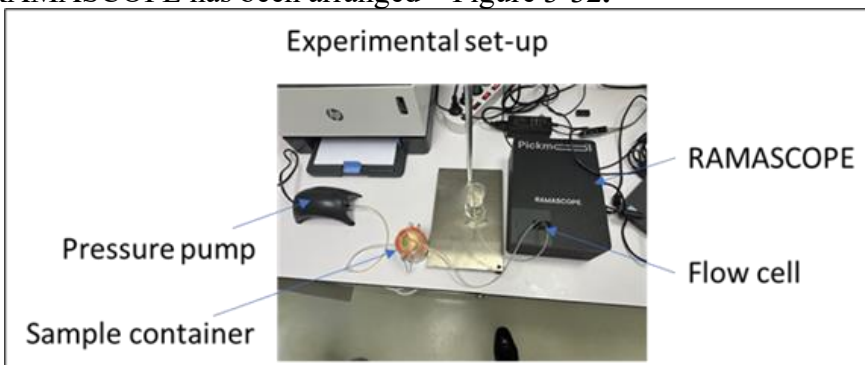


Figure 3-32: Experimental set-up for VOCs measurement by PickMol technology (SERS based)

3.4.4.3 Results

Such prepared and verified technology is currently tested for the detection of selected VOCs defined in WP1 (Table 3-7).

Table 3-7: VOCs defined in WP1 (by different color are marked molecules for which a specific type of functionalization could be used)

Pest	VOC name	VOC ID#	Cas Nr	chemical formula	Molecular mass (g/mol)	single VOC	1 VOC fomr ech pest	2 VOCs from reach pest
BMSB	(3S,6S,7R,10S)-10,11-Epoxy-1-bisabolene-3-ol	1		C ₁₅ H ₂₄ O ₂	232.36			
BMSB	(3R,6S,7R,10S)-10,11-Epoxy-1-bisabolene-3-ol	2		C ₁₅ H ₂₄ O ₂	232.36			
BMSB	(E)-2-Decenyl acetate	3	19487-61-7	C ₁₂ H ₂₀ O ₂	196.29			
BMSB	(E)-2-Decenal	4	3913-81-3	C ₁₀ H ₁₈ O	154.25			
BMSB	(E)-2-Hexenal	5	6728-26-3	C ₆ H ₁₀ O	98.14	BMSB	BMSB	BMSB
BMSB	(E)-2-Octenal	6	2548-87-0	C ₈ H ₁₄ O	126.20			BMSB
FAW	Dodecan-1-olacetate	7	112-53-8	C ₁₄ H ₂₈ O ₂	228.38			
FAW	7-Dodecen-1-olacetate	8	16677-06-8	C ₁₄ H ₂₆ O ₂	226.36			
FAW	11-Dodecen-1-olacetate	9	35153-10-7	C ₁₄ H ₂₆ O ₂	226.36			
FAW	Indole	10	120-72-9	C ₈ H ₇ N	117.15	FAW	FAW	FAW
FAW	Linalool	11	78-70-6	C ₁₀ H ₁₈ O	154.25			FAW
FAW	(Z)-3-Hexenyl acetate	12	3681-71-8	C ₈ H ₁₄ O ₂	142.20			
FAW	(E)-β-Farnesene	13	18794-84-8	C ₁₅ H ₂₄	204.36			
FAW	(3E)-4,8-Dimethyl-1,3,7-nonatriene	14	19945-61-0	C ₁₂ H ₂₀	164.29			
FAW	(3E,7E)-4,8,12-Trimethyl-1,3,7,11-tridecatetraene	15	62235-06-7	C ₁₅ H ₂₄	204.36			
CBW	Oleic acid	16	112-80-1	C ₁₈ H ₃₄ O ₂	282.47			
CBW	Palmitic acid	17	57-11-3	C ₁₆ H ₃₂ O ₂	256.44			
CBW	β-Myrcene	18	123-35-3	C ₁₀ H ₁₆	136.24			
CBW	β-Pinene	19	18172-67-3	C ₁₀ H ₁₆	136.24			CBW
CBW	D-Limonene	20	5989-27-5	C ₁₀ H ₁₆	136.24	CBW	CBW	CBW
CBW	(E)-Nerolidol	21	40716-66-3	C ₁₅ H ₂₆ O	222.37			
PHY	Ethanol	21	64-17-5	C ₂ H ₅ OH	46.07			PHY
PHY	3-Methyl-butanol	21	123-51-3	C ₅ H ₁₂ O	88.15			
PHY	2-Methyl-butanol	21	78-92-2	C ₅ H ₁₂ O	88.15	PHY	PHY	PHY
PHY	Phenylethyl alcohol	21	60-12-8	C ₈ H ₁₀ O	122.16			

PickMol technology is a tailored technology which means that for different molecules of interest (listed in the table) we have to prepare/develop a specific sensing chip. At this stage of the project implementation, we have decided to prepare a sensing chip for INDOLE detection.

To reach this goal three distinguished, but related activities must be performed:

- ✓ **SERS nanosensors surface morphology:** The first one is related with the exponential increment of the HS via the optimization of the shapes of silver/gold NPs which play a principal role in number of HS creation (see Figure 3-33– (a) – (e) different shapes and dimensions depending on physico-chemical conditions of preparation).

To reach this goal a series of experiments have been performed in which multiple physico-chemical parameters of created NPs with different morphology have been tested (temperature, pH, concentration of salts, position of plasmons resonance, morphology of NPs) with the aim to find the optimal shape and dimensions of NPs to produce plasmonic resonance in most suitable region.

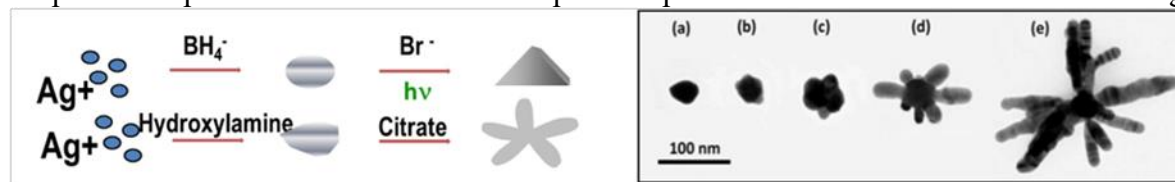


Figure 3-33: Different shapes of NPs depending on their preparation

SERS sensors functionalization: The second one is based on the NPs functionalization, which was carried out in the first stage with different kinds of organic linkers. Functionalization of nanoparticles with specific linkers aiming to increase a specific selectivity for the molecule of interest. These molecules allow an easy aggregation of new layers of Ag-NPs and the adsorption of VOCs: Thus, **i)** in the case if the size of VOCs enables them to enter in the matrix formed by the NPs, we will add new layers of NPs with different morphologies than the first one in order to raise both - the surface available for selected VOCs attachment and the number of HS in the colloidal solution, **ii)** in the case if the size of selected VOCs is too big for such arrangement of this matrix, we will anchor NPs with cavitands interacting with analytes by inclusion, contact or occlusion (e.g. cyclodextrins, calixarenes, carbon nanotubes or biomolecules) to act as VOCs receptor (see Figure 3-34).

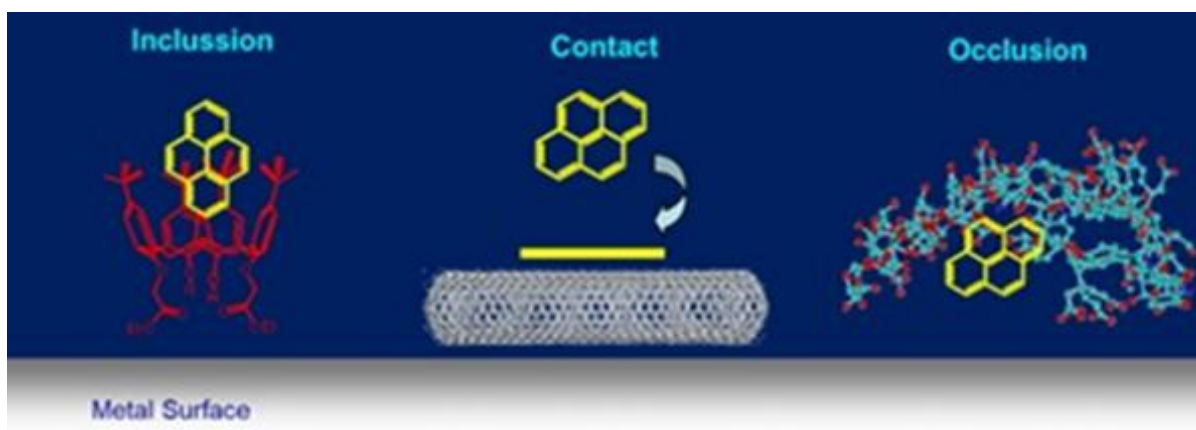


Figure 3-34: Principle of photonic sensor functionalization

- ✓ **SERS nanosensors optimization:** The third one is based on results from the previous two. We have constructed a final product – Biosensor chips for VOCs detection (INDOL in this case). The work has been organized in two closely related steps:
 - b) In the first step, we have produced silver and gold nanoparticles of different shapes (see step 1) which have been immobilized on a nanostructured substrate (silica/glass plates specifically covered by gold nano-shell). Depending on the type/shape of NPs deposited on the substrate and the distance between them, an optimum number of hot spots (HS) is created with a certain degree of specificity for a group of our target molecules (INDOL in this case).
 - b) In the second step, it was necessary to optimize the process of an application of the second layer of NPs of different shapes (see step 1) together with functionalization of the nanosurface/NPs by suitable linkers/cavitands (see step 2). The ultimate goal is to reach maximum reproducibility of the Raman signal, which is done by reaching homogeneity of the HS distribution on chip surface (see the next paragraph).

After multiple experiment described upstairs (different nanoparticles structure, different linkers, experiments with different excitation lines on laboratory Raman system etc.), we have decided to detect INDOLE in using nanoparticles shaped by a preparation of AgC (citrate colloid) and their functionalization by DT8 (1,8 - octanedithiol) – Figure 3-35. This type of SERS nanosensor preparation enables detecting volatile INDOLE molecules.

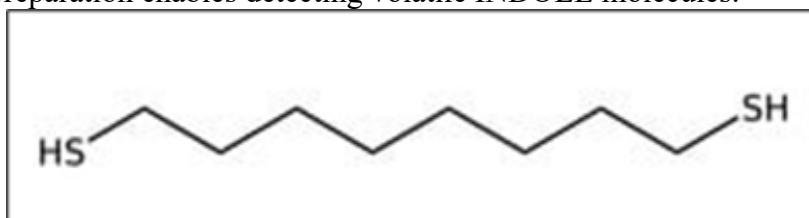


Figure 3-35: Structure of DT8 linker

The experimental set-up for the INDOLE detection by PickMol technology on developed tailored chip is presented in Figure 3-36. SAFTRA photonics is not equipped with any system measuring the concentration of VOCs. Thus, for the results presented in Figure 3-37 we cannot determine the concentration of INDOLE. The experiments were performed in an experimental set up described in Figure 3-36 and for protection (INDOLE is a toxic substance) all parts of the experimental arrangement were placed into a hood. SERS spectra of INDOLE and their time development are presented in Figure 3-37.



Figure 3-36: Experimental set-up for detection of INDOLE molecules

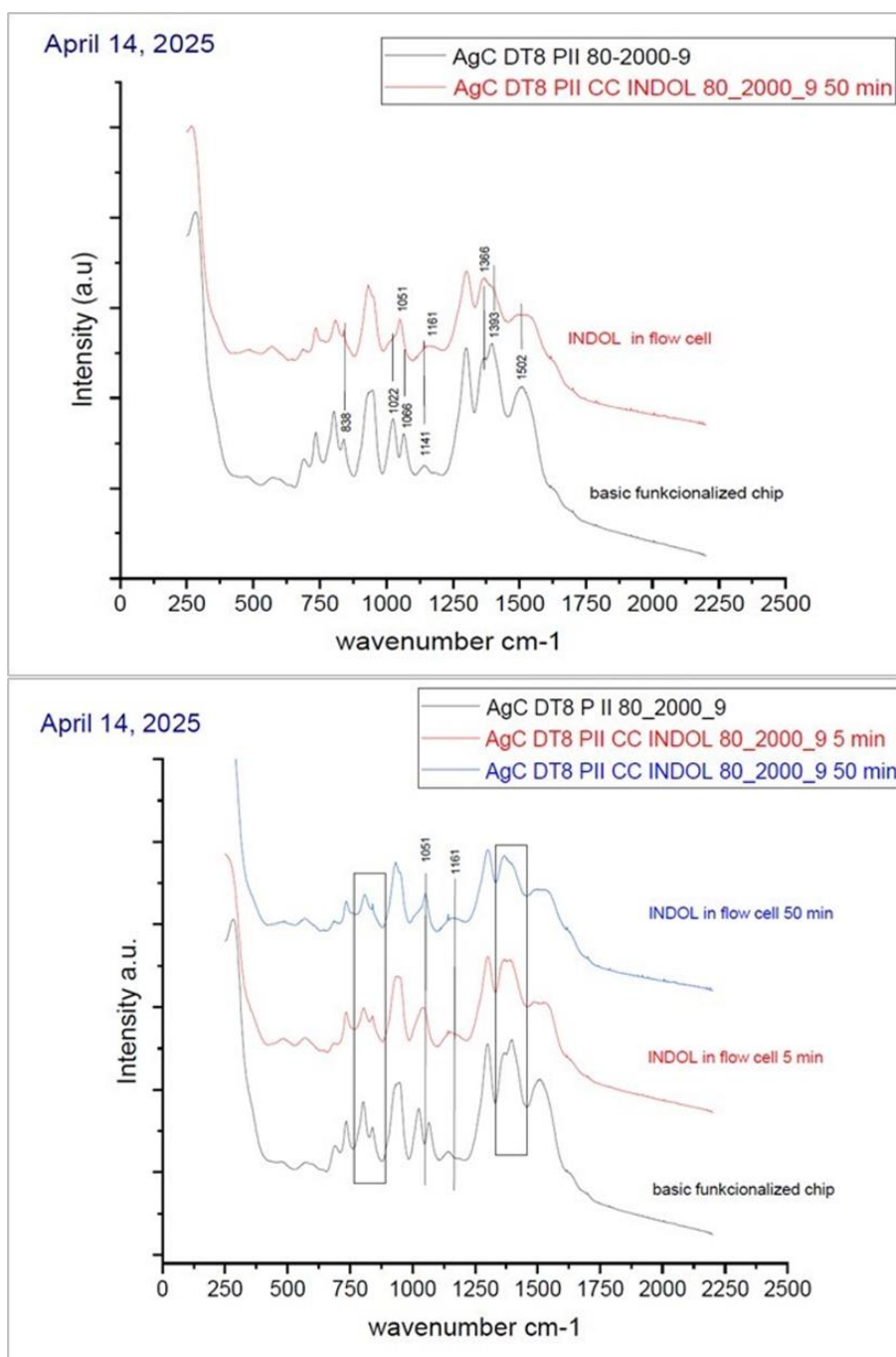


Figure 3-37: SERS spectra of INDOLE (top), time development of the spectra (bottom)

The main feature observed in the spectra is the disappearing of doublet at 1022 and 1066 cm^{-1} transformed into a single band at 1051 cm^{-1} , other changes caused by interaction of INDOLE with the nanosurface of functionalized chip are: intensity decrease of the band at 838 cm^{-1} , shift of the band at 1141 cm^{-1} , to the position at 1161 cm^{-1} , intensity decrease of the band at 1502 cm^{-1} , and finally change of relative intensity ratio of doublet at 1366 and 1393 cm^{-1} .

Interpretation of spectral changes: The interpretation of observed changes will need some deeper look into possible changes in structures of DT8 as well as INDOLE caused by their mutual interaction. For the moment we can interpret selected spectral features. The doublet at 730/620 corresponds to the C-S bond of DT8, where the 730 cm^{-1} band is due to the trans conformation, whereas the 620 cm^{-1} one corresponds to the gauche conformation. As indole is injected, the trans component seems to increase due to the interaction with the ligand while the gauche band is decreasing. This means that the DT8 chains increase their ordered conformation upon interaction with indole.

The same occurs on the 1066/1022 doublet. The first is attributed to ordered (trans) C-C bonds in aliphatic chains, while the 1022 cm^{-1} one is due to disordered CC bonds (gauche). Again, an increase of ordered conformations (1050-1060 cm^{-1}) is seen after injecting indole on the chip.

There is a small band at about 1520 cm^{-1} that may correspond directly to indole (the highest Raman band of indole).

We will prepare a more detailed spectra interpretation in the next step.

After 50 min of continuous flow of INDOLE through flow cell with tailored PickMol chip, one can see even slightly more profound changes of mentioned spectra variation (Figure 3-37 bottom figure). This could indicate that PickMol chip has been already highly saturated by INDOLE even at the time zero (beginning of the experiment). It is proposed to verify this hypothesis by using a concentration control system (collaboration with SINTEF).

3.4.4.4 Conclusions

1. After all the work described above, we were capable of detecting one molecule from the list of VOCs. The problem of quantitative calibration remains to be answered, which is a task that we need to solve in cooperation within the project.
2. It was shown that (in principle) SERS technology could be used for the detection of selected VOCs, by developing tailored chips.
3. The integration of the technology into a complex SSP system and/or its specific use as a complementary technology in case of need for detection of specific VOCs substances is proposed to be discussed.

4 CONCLUSION

The functional testing of the first SSPs has demonstrated significant progress in the development of portable, sensitive, and selective VOC detection systems for pest monitoring in agriculture. Key findings include:

- **AIRMO's heated PID** and gradient oven significantly improved detection of high-boiling-point VOCs, addressing limitations of earlier prototypes.
- **VOLATILE's Scout3 system** proved to be a robust benchmarking tool, with flexible integration options for emerging sensor technologies.
- **UWAR's μ -GC and SMR systems** showed promising results in VOC separation and detection, with high accuracy in compound classification using machine learning models.
- **SINTEF's SURMOF coatings and SERS substrates** revealed potential for enhanced selectivity, though further reproducibility improvements are needed.
- **SAFTRA's PickMol technology** successfully detected indole, validating the feasibility of tailored SERS chips for specific VOCs.

5 REFERENCES

[1] Usman Yaqoob, Siavash Esfahani, Marina Cole, Julian W. Gardner, “3D Printed Micro-Gas Chromatography (μ -GC) System for Improved Low-Cost VOC sensing.”, Eurosensors 2024, DOI 10.5162/EUROSENSORSXXXVI/PT5.230.

[2] Usman Yaqoob, Siavash Esfahani, Marina Cole, Julian W. Gardner, “Design of low-cost 3D printed micro-gas chromatography (μ -GC) column for fast VOC analysis”, accepted in IMCS 2025.

[3] Usman Yaqoob, Dylan Limbani, Siavash Esfahani, Marina Cole, Julian W. Gardner, “3D-Printed μ -GC Integrated with an E-Nose System for Enhanced Plant Health Prediction” accepted in Eurosensors 2025.

[4] Bulk Acoustic Wave Resonator Based Sensor - Patent No.: US 11,249,049 B2

[5] Particle-Sensing Device; British Patent No.: GB2599099; European Patent App. No.21782793.0; US Patent App. 18/246,409

[6] Usman Yaqoob, Barbara Urasinska-Wojcik, Siavash Esfahani, Marina Cole, Julian W. Gardner, “Rapid Detection of Linalool Using Solidly Mounted Resonators for Plant Health Monitoring” accepted in Eurosensors 2025.

[7] Usman Yaqoob, Barbara Urasinska-Wojcik, Siavash Esfahani, Marina Cole, Julian W. Gardner, “Rapid and Selective Detection of Linalool Using SMRs for Plant Health Monitoring” submitted in IEEE Sensors Journal.